International Journal of Bifurcation and Chaos

TRANSITION FROM PARTIAL TO GLOBAL GENERALIZED SYNCHRONIZATION IN NETWORKS OF STRUCTURALLY DIFFERENT TIME-DELAY SYSTEMS

R. Suresh[1], D. V. Senthilkumar[1], M. Lakshmanan[2*], and J. Kurths[3,4,5]
[1]*Centre for Nonlinear Science & Engineering, School of Electrical & Electronics Engineering, SASTRA University, Thanjavur - 613 402, India.*

[2]*Centre for Nonlinear Dynamics, School of Physics, Bharathidasan University, Tiruchirapalli - 620 024, India*
*lakshman@cnld.bdu.ac.in

[3]*Potsdam Institute for Climate Impact Research, Telegraphenberg, Potsdam D-14473, Germany*

[4]*Institute of Physics, Humboldt University, Berlin D-12489, Germany*

[5]*Institute for Complex Systems and Mathematical Biology, University of Aberdeen, Aberdeen AB24 3FX, United Kingdom*

Received (to be inserted by publisher)

We point out the existence of transition from partial to global generalized synchronization (GS) in symmetrically coupled regular networks (array, ring, global and star) of distinctly different time-delay systems of different orders using the auxiliary system approach and the mutual false nearest neighbor method. It is established that there exist a common GS manifold even in an ensemble of structurally nonidentical time-delay systems with different fractal dimensions and we find that GS occurs simultaneously with phase synchronization (PS) in these networks. We calculate the maximal transverse Lyapunov exponent to evaluate the asymptotic stability of the complete synchronization manifold of each of the main and the corresponding auxiliary systems, which, in turn, ensures the stability of the GS manifold between the main systems. Further we also estimate the correlation coefficient and the correlation of probability of recurrence to establish the relation between GS and PS. We also deduce an analytical stability condition for partial and global GS using the Krasovskii-Lyapunov theory.

Keywords: partial generalized synchronization; global generalized synchronization, structurally different time-delay systems; networks of time-delay systems.

1. Introduction

In the last two decades, the phenomenon of chaos synchronization has been extensively studied in coupled nonlinear dynamical systems from both theoretical and application perspectives due to its significance

*Author for correspondence

in diverse natural and man-made systems [Pikovsky *et al.*, 2001; Lakshmanan & Senthilkumar, 2010]. In particular, various types of synchronization, namely complete synchronization (CS), phase synchronization (PS), intermittent lag/anticipatory synchronizations and generalized synchronization (GS) have been identified in coupled systems. All these types of synchronization have been investigated mainly in identical systems and in systems with parameter mismatch. Very occasionally it has been studied in distinctly non-identical (structurally different) systems. But in reality, structurally different systems are predominant in nature and very often the phenomenon of synchronization (GS) is responsible for their evolutionary mechanism and proper functioning of such distinctly nonidentical systems. As typical examples, we may cite the cooperative functions of brain, heart, liver, lungs, limbs, etc., in living systems and coherent coordination of different parts of machines, between cardiovascular and respiratory systems [Schafer *et al.*, 1998], different populations of species [Blasius *et al.*, 1999; Amritkar & Rangarajan, 2006], in epidemics [Grenfell *et al.*, 2001; Earn *et al.*, 1998], in visual and motor systems [Famer, 1998; Sebe *et al.*, 2006], in climatology [Stein *et al.*, 2011; Maraun & Kurths, 2005], in paced maternal breathing on fetal [Van Leeuwen *et al.*, 2009] etc. It has also been shown that GS is more likely to occur in spatially extended systems and complex networks (even in networks with identical nodes, due to the large heterogeneity in their nodal dynamics) [Shang *et al.*, 2009; Hung *et al.*, 2008; Moskalenko *et al.*, 2012]. In addition, GS has been experimentally observed in laser systems [Uchida *et al.*, 2003], liquid crystal spatial light modulators [Rogers *et al.*, 2004], microwave electronic systems [Dmitriev *et al.*, 2009] and has applications in secure communication devices [Murali & Lakshmanan, 1998; Moskalenko *et al.*, 2010]. Therefore understanding the evolutionary mechanisms of many natural systems necessitates the understanding of the intricacies involved in the underlying generalized synchronization (GS) phenomenon.

The phenomenon of GS has been well studied and understood in unidirectionally coupled systems [Kocarev & Parlitz, 1996; Rulkov *et al.*, 1995; Abarbanel *et al.*, 1996; Brown, 1998; Pyragas, 1996], but still it remains largely unexplored in mutually coupled systems. Only a limited number of studies are available on GS in mutually coupled systems even with parameter mismatches [Zheng *et al.*, 2002; Hung *et al.*, 2008; Guan *et al.*, 2009; Chen *et al.*, 2009; Hu *et al.*, 2010; Guan *et al.*, 2010; Shang *et al.*, 2009; Moskalenko *et al.*, 2012; Shahverdiev & Shore, 2009; Acharyya & Amritkar, 2013] and rarely in structurally different dynamical systems with different fractal dimensions [Boccaletti *et al.*, 2000]. Recent investigations have revealed that GS emerges even in symmetrically (mutually) coupled network motifs in networks of identical systems, and that it also plays a vital role in achieving coherent behavior of the entire network [Soriano *et al.*, 2012; Moskalenko *et al.*, 2012]. As almost all natural networks are heterogeneous in nature, the notion of GS has been shown to play a vital role in their evolutionary mechanisms [Pikovsky *et al.*, 2001]. Thus to unravel the role of GS in such large networks, it is crucial to understand the emergence of GS in heterogeneous network motifs composed of distinctly different nonidentical systems. It is to be noted that the notion of PS has been widely investigated in mutually coupled essentially different (low-dimensional) chaotic systems [Pikovsky *et al.*, 2001], while the notion of GS in such systems has been largely ignored. It is an accepted fact that PS is weaker than GS (because PS does not add restrictions on the amplitude, and only the locking of the phases is crucial). Parlitz et al. have shown that in general GS always leads to PS, if one can suitably define a phase variable, and that GS is stronger (which has been studied in unidirectionally coupled chaotic systems). That is, PS may occur in cases where the coupled systems show no GS [Parlitz *et al.*, 1996]. Further, the transition from PS to GS as a function of the coupling strength has been demonstrated in coupled time-delay systems with parameter mismatch which confirms that PS is weaker than GS [Senthilkumar *et al.*, 2007]. On the other hand, Zhang and Hu [Zheng & Hu, 2000] have demonstrated that GS is not necessarily stronger than PS, and in some cases PS comes after GS with increasing coupling strength depending upon the degree of parameter mismatch. They have concluded that PS (GS) emerges first for low (high) degree of parameter mismatch and that they both occur simultaneously for a critical range of mismatch in low-dimensional systems [Zheng & Hu, 2000]. In general, the notion of GS and its relation with PS in mutually coupled systems, particularly in distinctly nonidentical systems with different fractal dimensions including time-delay systems, need much deeper understanding.

In line with the above discussion, we have reported briefly the existence of GS in symmetrically coupled networks of distinctly nonidentical time-delay systems using the auxiliary system approach in a letter

[Senthilkumar *et al.*, 2013]. In this paper, we will provide an extended version of the letter with important additional results and explanations. In particular, in this paper we will demonstrate the occurrence of a transition from partial to global GS in mutually coupled networks of structurally different time-delay systems (for $N = 2$, 3 and 4) with different fractal (Kaplan-Yorke) dimensions and in systems with different orders using the auxiliary system approach and the mutual false nearest neighbor (MFNN) method. We use the Mackey-Glass (MG) [Mackey & Glass, 1977], a piecewise linear (PWL) [Senthilkumar *et al.*, 2006, 2007], a threshold piecewise linear (TPWL) [Suresh *et al.*, 2013] and the Ikeda time-delay [Ikeda *et al.*, 1980] systems to construct heterogeneous network motifs. The main reason to consider time-delay systems in this study is that even with a single time-delay system, one has the flexibility of choosing systems with different fractal dimensions just by adjusting their intrinsic delay alone, which is a quite attracting feature of time-delay systems from modelling point of view [Appeltant *et al.*, 2011]. Further, time-delay systems are ubiquitous in several real situations, including problems in ecology, epidemics, physiology, physics, economics, engineering and control systems, [Lakshmanan & Senthilkumar, 2010] which inevitably require delay for a complete description of the system (note that intrinsic delay is different from connection delays which arise between different units due to finite signal propagation time).

In our present work, we report that there exists a common GS manifold even in networks of distinctly different time-delay systems. In other words, there exists a functional relationship even for systems with different fractal dimensions, which maps them to a common GS manifold. Further, we also wish to emphasize that our results are not confined to just scalar one-dimensional time-delay systems alone but we confirm that there exists a similar type of synchronization transitions even in the case of time-delay systems of different orders. Particularly, we demonstrate that synchronization phenomenon occurs in a system of a Ikeda time-delay system (first order time-delay system) mutually coupled with a Hopfield neural network (a second order time-delay system), and in a system of a MG time-delay system (first order time-delay system) mutually coupled with a plankton model (a third order system with multiple delays) to establish the generic nature of our results. Stability of GS manifold in unidirectionally coupled systems is usually determined by examining the conditional Lyapunov exponents of the synchronization manifold [Kocarev & Parlitz, 1996; Pyragas, 1996] or the Lyapunov exponents of the coupled system itself [Moskalenko *et al.*, 2012]. Here, we will estimate the maximal transverse Lyapunov exponent (MTLE) to determine the asymptotic stability of the CS manifold of each of the systems with their corresponding auxiliary systems starting from different initial conditions, which in turn asserts the stability of GS between the original distinctly nonidentical time-delay systems. Further, we will also estimate the cross correlation (CC) and the correlation of probability of recurrence (CPR) to establish the relation between GS and PS (here GS and PS always occur simultaneously in structurally different time-delay systems). CC essentially gives a much better statistical average of the synchronization error, which is being widely studied to characterize CS. Further, CPR is a recurrence quantification tool [Marwan *et al.*, 2007], which effectively characterizes the existence of PS especially in highly non-phase-coherent hyperchaotic attractors usually exhibited by time-delay systems [Senthilkumar *et al.*, 2006]. It is also to be noted that the auxiliary system approach has some practical limitations. This method fails for systems whose dynamical equations are not known. Particularly, CS between response and auxiliary systems arises only when their initial conditions are set to be in the same basin of attraction. Due to the above limitations of the auxiliary system approach, we have also calculated the mutual false nearest neighbor (MFNN) which doubly confirms our results. In addition, an analytical stability condition using the Krasovskii-Lyapunov theory is also deduced in suitable cases.

The remaining paper is organized as follows: In Sec. 2, we will describe briefly the notion of structurally different time-delay systems with different fractal dimensions with examples. In Secs. 3 and 4, we will demonstrate the existence of a transition from partial to global GS in $N = 2$ mutually coupled time-delay systems using the auxiliary system approach and the MFNN method, respectively. An analytical stability condition is also deduced using the Krasovskii-Lyapunov theory in Sec. 3. The transition from partial to global GS is demonstrated in $N = 3$ mutually coupled time-delay systems with an array and a ring coupling configuration in Sec. 5. In Sec. 6, we will consider $N = 4$ mutually coupled time-delay systems with array, ring, global and star configurations and discuss the occurrence of partial and global GS. The above synchronization transition in time-delay systems with different orders is demonstrated in Sec. 7 and finally we summarize our results in Sec. 8.

2. Structurally Different Time-delay Systems with Different Fractal Dimensions

In this section, we consider structurally different first order scalar time-delay systems with different fractal dimensions. Here, structurally different time-delay systems refer to systems exhibiting chaotic/hyperchaotic attractors with different phase space geometry characterized by different degree of complexity. Despite the similarity in the structure of the evolution equations, the nature of chaotic attractors, the number of positive LEs and their magnitudes characterizing the rate of divergence and the degree of complexity as measured by the Kaplan-Yorke dimension (D_{KY}) of the underlying dynamics are different even for the same value of time-delay because of the difference in the nonlinear functional form.

As an illustration, first let us consider a symmetrically coupled arbitrary network of distinctly non-identical scalar time-delay systems. Then the dynamics of the ith node in the network is represented as

$$\dot{\mathbf{x}}_i = -\alpha_i \mathbf{x}_i(t) + \beta_i \mathbf{f}_i(\mathbf{x}_i(t-\tau_i)) - \varepsilon \sum_{j=1}^{N} G_{ij}\mathbf{x}_j, \tag{1}$$

where $i = 1, ..., N$, and N is the number of nodes in the network, α_i's and β_i's are system's parameters, τ_i's the time-delays, the nonlinear function of the ith node is defined as $\mathbf{f}_i(\mathbf{x}_i)$, ε is the coupling strength and G a Laplacian matrix which determines the topology of the arbitrary network. For the MG time-delay system, we choose the nonlinear function defined as [Mackey & Glass, 1977]

$$f_1(x(t-\tau_1)) = \frac{x_1(t-\tau_1)}{(1+(x_1(t-\tau_1)^{10}))}, \tag{2}$$

and for the PWL system with the nonlinear function given as [Senthilkumar *et al.*, 2006, 2007]

$$f_2(x) = \begin{cases} 0, & x \le -4/3 \\ -1.5x-2, & -4/3 < x \le -0.8 \\ x, & -0.8 < x \le 0.8 \\ -1.5x+2, & -0.8 < x \le 4/3 \\ 0, & x > 4/3. \end{cases} \tag{3}$$

For the TPWL system we choose the form of the nonlinear function as given by [Suresh *et al.*, 2013]

$$f_3(x) = AF^* - Bx, \tag{4}$$

with

$$F^* = \begin{cases} -x^*, & x < -x^* \\ x, & -x^* \le x \le x^* \\ x^*, & x > x^*, \end{cases} \tag{5}$$

and for the Ikeda time-delay system the nonlinear function is given by [Ikeda *et al.*, 1980]

$$f_4(x(t-\tau_4)) = sin(x(t-\tau_4)). \tag{6}$$

The parameter values for the above time-delay systems are chosen throughout the paper as follows:
1) For the MG systems: We choose $\beta_1 = 0.5$, $\alpha_1 = 1.0$, and $\tau_1 = 8.5$;
2) For the PWL systems: We choose $\beta_2 = 1.0$, $\alpha_2 = 1.2$, $\tau_2 = 10.0$, $p_1 = 0.8$ and $p_2 = 1.33$;
3) The parameter values for the TPWL are fixed as $\beta_3 = 1.0$, $\alpha_3 = 1.2$, $\tau_3 = 7.0$, $A = 5.2$, $B = 3.5$ and $x^* = 0.7$ and
4) for the Ikeda time-delay system we choose $\beta_4 = 1.0$, $\alpha_4 = 5.0$, $\tau_4 = 7.0$. The hyperchaotic attractors of the uncoupled MG, PWL, TPWL and Ikeda time-delay systems are depicted in Figs. 1(a)-(d), respectively. The first few largest LEs of all the above four (uncoupled) time-delay systems are shown as a function of the delay time τ in Figs. 2(a)-(d). It is also clear from this figure that the number of positive LEs, and

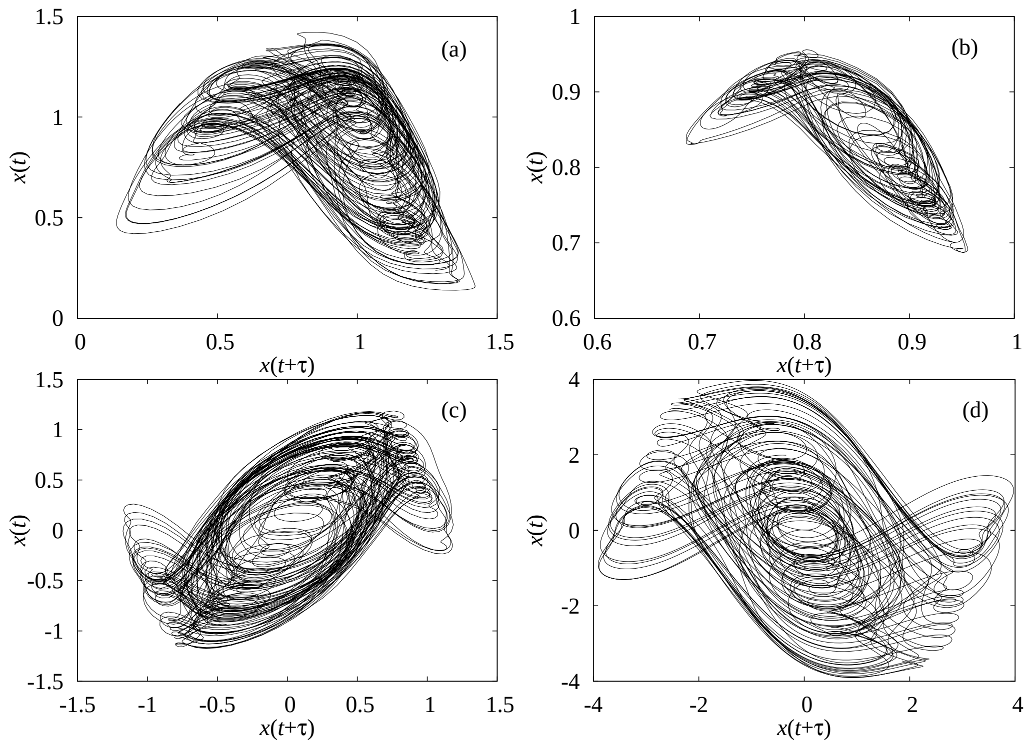

Fig. 1. Hyperchaotic attractors of (a) Mackey-Glass,(b) piecewise linear (PWL), (c) piecewise linear with threshold nonlinearity (TPWL) and (d) Ikeda time-delay systems for the choice of parameters given in Table 1.

hence the complexity and dimension of the state space, generally increase with the delay time. Further, the degree of complexity, measured by their number of positive LEs of the dynamics (attractors) exhibited by all the four systems are distinctly different even for the same value of time-delay. In fact, we have taken different values of delay for each of the systems, as pointed out by the arrows in Fig. 2, to demonstrate the existence of suitable smooth transformation that maps the strongly distinct individual systems to a common GS manifold.

Table 1. The parameter values, number of positive LEs and Kaplan-Yorke dimension (D_{ky}) of the structurally different time-delay systems.

No	System	Choice of parameters			No. of Positive LEs	D_{ky}
		β_i	α_i	τ_i		
1	MG	0.5	1.0	8.5	2	2.957
2	PWL	1.0	1.2	10.0	3	4.414
3	TPWL	1.0	1.2	7.0	4	8.211
4	Ikeda	1.0	5.0	7.0	5	10.116

We wish to emphasize especially the structural difference, measured by their degree of complexity, between the hyperchaotic attractors of different scalar first order time-delay systems (Fig. 1) which we have studied in this paper and are detailed in Table 1: 1) the MG system has two positive LEs with $D_{KY} = 2.957$ for $\tau_1 = 8.5$, 2) the PWL time-delay system has three positive LEs with $D_{KY} = 4.414$ for $\tau_2 = 10.0$, 3) the TPWL time-delay system has four positive LEs with $D_{KY} = 8.211$ for $\tau_3 = 7.0$ and 4) the Ikeda system has five positive LEs with $D_{KY} = 10.116$ for $\tau_4 = 7.0$. The above facts clearly indicate that the real state space dimension explored by the flow of a time-delay system, which is essentially infinite-dimensional in nature, and the associated degree of complexity are characterized by the form of

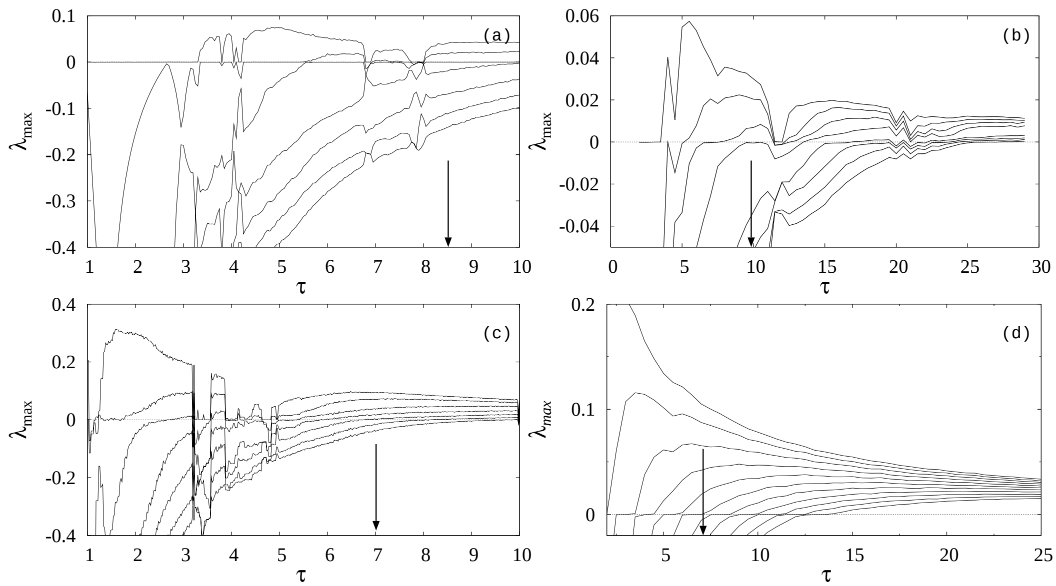

Fig. 2. First few largest Lyapunov exponents of (a) Mackey-Glass,(b) piecewise linear (PWL), (c) piecewise linear with threshold nonlinearity (TPWL) and (d) Ikeda time-delay systems, as a function of the time-delay. Arrows point the value of the delay time we have considered in our analysis.

nonlinearity and the value of delay time irrespective of the similarity of the underlying evolution equations of the scalar first order time-delay systems.

3. Transition from Partial to Global GS in Mutually Coupled Time-delay Systems: Auxiliary System Approach

It has already been shown that the functional relationship between two different systems in GS is generally difficult to identify analytically. However GS in such systems can be characterized numerically using various approaches, namely the mutual false nearest neighbor method [Rulkov *et al.*, 1995], the statistical modeling approach [Schumacher *et al.*, 2012], the phase tube approach [Koronvskii *et al.*, 2011], the auxiliary system approach [Abarbanel *et al.*, 1996], etc. Among all these methods the auxiliary system approach is extensively used to detect the presence of GS in unidirectionally coupled systems (both in numerical and experimental studies due to its simple and powerful implementation). Abarbanel et al. [Abarbanel *et al.*, 1996] first introduced this approach to characterize and confirm GS in dynamical systems (when the system equations are known). The mathematical formulation of this concept was put forward by Kocarev and Parlitz [Kocarev & Parlitz, 1996] for a drive-response configuration in low-dimensional systems. They formulated it as the asymptotic convergence of the response and its auxiliary systems which are identically coupled to the drive system, starting from two different initial conditions from the same basin of attraction. The asymptotic convergence indeed ensures the existence of an attracting synchronization manifold (CS manifold between the response and auxiliary systems and GS manifold between the drive and response systems) [Kocarev & Parlitz, 1996]. In other words, GS between the drive $\mathbf{x}$ and the response $\mathbf{y}$ systems occur only when the response system is asymptotically stable, that is $\forall\ \mathbf{y_i}(0)$ & $\mathbf{x}(0)$ in the basin of the synchronization manifold one requires $\lim_{t\to\infty} ||\mathbf{y}(t,\mathbf{x}(0),\ \mathbf{y}_1(0)) - \mathbf{y}(t,\mathbf{x}(0),\ \mathbf{y}_2(0))|| = 0$.

Now, we will provide an extension of this approach to a network for mutually coupled systems. For simplicity, we consider two mutually coupled nonidentical distinctly different time-delay systems represented by

$$\dot{\mathbf{x}} = \mathbf{f}(\mathbf{x},\ \mathbf{x}_\tau,\ \mathbf{u}), \quad \text{and} \tag{7a}$$

$$\dot{\mathbf{y}} = \mathbf{g}(\mathbf{y},\ \mathbf{y}_\tau,\ \mathbf{v}), \qquad \mathbf{f} \neq \mathbf{g} \tag{7b}$$

where $\mathbf{x},\ \mathbf{x}_\tau \in \mathbf{R}^n,\ \mathbf{y},\ \mathbf{y}_\tau \in \mathbf{R}^m$, $\tau \in \mathbf{R}$ $(\mathbf{x}_\tau = \mathbf{x}(\mathbf{t}-\tau),\ \mathbf{y}_\tau = \mathbf{y}(\mathbf{t}-\tau))$ and $\mathbf{u},\ \mathbf{v} \in \mathbf{R}^k,\ k \leq m,\ n$. $u_i = -v_i = h_i\left(\mathbf{x}(t,\mathbf{x}_0),\ \mathbf{y}(t,\mathbf{y}_0)\right)$ correspond to the driving signals. System (7) is in GS if there exists a transformation $\mathbf{H}$ such that the trajectories of the systems (7a) and (7b) are mapped onto a subspace (synchronization manifold) of the whole state space $\mathbf{R}^n \times \mathbf{R}^m$. That is

$$\mathbf{H} : (\mathbf{R}^n, \mathbf{R}^m) \rightarrow \mathbf{R}^\mu \subset \mathbf{R}^n \times \mathbf{R}^m. \tag{8}$$

We also note here that since we are dealing with GS of nonidentical systems with different fractal dimensions, the transformation function $\mathbf{H}$ refers to a generalized transformation (not identity transformation) and also there may exist a set of transformations $\mathbf{H}$ that maps a given $\mathbf{x},\ \mathbf{x}_\tau \in \mathbf{R}^n$ and $\mathbf{y},\ \mathbf{y}_\tau \in \mathbf{R}^m$ to different subspaces of $\mathbf{R}^\mu$. This indicates that the synchronization manifold $M = \{(\mathbf{x},\ \mathbf{y}) : \mathbf{H}(\mathbf{x},\ \mathbf{y}) = 0\}$ is such that $\forall\ \mathbf{x}(\hat{\tau}), \mathbf{y}(\hat{\tau}), \hat{\tau} \in [-\tau, 0]$, which lies within a subset of the basin of attraction $B = B_\mathbf{x} \times B_\mathbf{y} \equiv \mathbf{R}^\mu$, approaches $M \subset B$, so that M is an attracting manifold. Here $B_\mathbf{x}$ and $B_\mathbf{y}$ are the basins of attraction of systems (7a) and (7b), respectively. The synchronization manifold M could also be

$$M = \{(\mathbf{x},\ \mathbf{y}) : \mathbf{y} = \mathbf{H}(\mathbf{x})\} \text{ or } M = \{(\mathbf{x},\ \mathbf{y}) : \mathbf{x} = \mathbf{H}(\mathbf{y})\} \tag{9}$$

as special cases, but without ambiguity $M = \mathbf{H}(\mathbf{x},\ \mathbf{y})$ is the most general one for mutually coupled systems. Hence, GS exists between the systems (7a) and (7b) only when both coupled systems are asymptotically stable. That is, $\forall\ (\mathbf{x}_i(\hat{\tau}),\ \mathbf{y}_i(\hat{\tau})),\ \hat{\tau} \in [-\tau, 0] \subset B,\ i = 1, 2$, one requires

$$\lim_{t\to\infty} ||\mathbf{y}(t, \mathbf{x}_1(\hat{\tau}),\ \mathbf{y}_1(\hat{\tau})) - \mathbf{y}(t, \mathbf{x}_1(\hat{\tau}),\ \mathbf{y}_2(\hat{\tau}))|| = 0, \tag{10a}$$

$$\lim_{t\to\infty} ||\mathbf{x}(t, \mathbf{x}_1(\hat{\tau}),\ \mathbf{y}_1(\hat{\tau})) - \mathbf{x}(t, \mathbf{x}_2(\hat{\tau}),\ \mathbf{y}_1(\hat{\tau}))|| = 0 \tag{10b}$$

Further, it is worth to emphasize that in Ref. [Parlitz *et al.*, 1997], it is reported that a subharmonic entrainment takes place when there exists a relation between the interacting systems, which usually takes place for periodic synchronization with $m : n$ periods, $m \neq n$. But in this paper, the synchronization dynamics in all the cases we have considered exhibits chaotic/hyperchaotic oscillations and hence the transformation function H refers to the existence of a function (not a relation) in our case. Therefore the trajectories of Eq. (7) starting from the basin of attraction B asymptotically reach the synchronization manifold M defined by the transformation function $\mathbf{H}(\mathbf{x}, \mathbf{y})$, which can be smooth if the systems (7) uniformly converge to GS manifold (otherwise nonsmooth). The uniform convergence (smooth transformation) is confirmed by negative values of their local Lyapunov exponents of the synchronization manifold M [Pecora *et al.*, 1997].

Now, we will demonstrate the existence of GS in symmetrically coupled arbitrary networks of distinctly nonidentical time-delay systems with different fractal dimensions using the auxiliary system approach. We consider a symmetrically coupled arbitrary network as given in Eq. (1). To determine the asymptotic stability of each of the nodes in this network, one can define a network (auxiliary) identical to Eq. (1) (starting from different initial conditions in the same basin of attraction), whose node dynamics is represented as

$$\dot{\mathbf{x}}'_i = -\alpha_i \mathbf{x}'_i(t) + \beta_i \mathbf{f}'_i(\mathbf{x}'_i(t - \tau_i)) - \varepsilon \sum_{j=1}^{N} G_{ij}(\mathbf{x}_j - \delta_{ij}\mathbf{x}_j). \tag{11}$$

The parameter values are the same as in Eq.(1) discussed in Sec. 2. In the following sections, we will investigate the existence of transition from partial GS to global GS in networks of $N = 2, 3$ and 4 systems with a linear array, ring, global and star coupling configurations.

3.1. $N = 2$ *mutually coupled systems*

To start with, in order to demonstrate the existence of GS between two ($N = 2$) mutually coupled nonidentical distinctly different time-delay systems, we consider the network given in Fig. 3(a). Here 1 and 2 are mutually coupled distinctly nonidentical time-delay systems and $1'$ and $2'$ are the associated auxiliary systems. Fig. 3 also depicts schematically different configurations for $N > 2$, which are discussed later on. The state equations for $N = 2$ coupled systems can be represented as

$$\dot{x}_1 = -\alpha_1 x_1(t) + \beta_1 f_1(x_1(t - \tau_1)) + \varepsilon(x_2 - x_1), \tag{12a}$$

$$\dot{x}_2 = -\alpha_2 x_2(t) + \beta_2 f_2(x_2(t - \tau_2)) + \varepsilon(x_1 - x_2). \tag{12b}$$

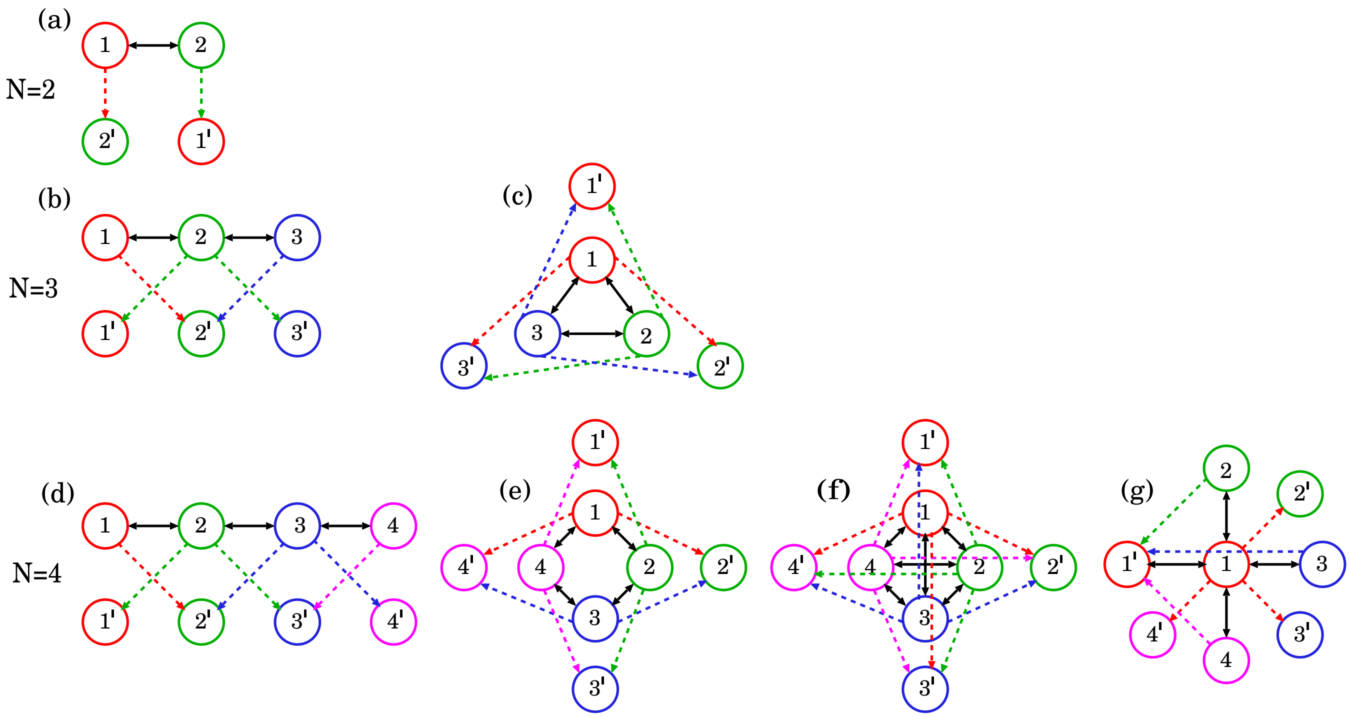

Fig. 3. Schematic diagrams of the auxiliary system approach for networks of mutually coupled systems. (a, b, d) Linear arrays with $N = 2,\ 3,\ 4$, (c, e) ring configurations with $N = 3,\ 4$, and (f, g) global and star coupling configurations with $N = 4$.

Now, let us couple the auxiliary system $1'$ to 2 and $2'$ to 1 unidirectionally as given in Fig. 3(a), such that the systems 1 and $1'$ are driven by the same signal from system 2, and systems 2 and $2'$ are similarly driven by system 1. The corresponding dynamical equation for the auxiliary systems can be given as

$$\dot{x}_1' = -\alpha_1 x_1'(t) + \beta_1 f_1'(x_1'(t-\tau_1)) + \varepsilon(x_2 - x_1'), \tag{13a}$$

$$\dot{x}_2' = -\alpha_2 x_2'(t) + \beta_2 f_2'(x_2'(t-\tau_2)) + \varepsilon(x_1 - x_2'). \tag{13b}$$

We choose the MG time-delay systems (system 1 and $1'$) with the nonlinear function $f_1(x)$ given in Eq. (2) and the PWL systems (system 2 and $2'$) with the nonlinear function $f_2(x)$ given in Eq. (3). The parameters of both systems are fixed as given in Sec. 2 (Table 1) and for those parameter values both systems exhibit hyperchaotic attractors [Figs. 1(a) and 1(b)] with two [Fig. 2(a)] and three [Fig. 2(b)] positive LEs, respectively.

Generally, in mutual coupling configuration the systems affect each other and attain a common synchronization manifold simultaneously above a threshold value of the coupling strength. But interestingly in distinctly different coupled time-delay systems with different fractal dimensions, one of the systems first reaches the GS manifold for a lower value of ε, while the other system remains in a desynchronized state, which we call as a partial GS state. For a further increase of ε both systems organize themselves and enter into a common GS manifold, thereby achieving a global GS. In other words, when system 1 and $1'$ are identically synchronized, system 1 is synchronized to a subspace (synchronization manifold) of the whole state space $\mathbf{R}^n \times \mathbf{R}^m$ of both systems in a generalized sense, which we call as a partial GS. Similarly, when the systems 2 and $2'$ are synchronized identically, then system 2 is synchronized to the common synchronization manifold. This corroborates that both systems 1 and 2 share a common GS manifold in the phase space $\mathbf{R}^n \times \mathbf{R}^m$. Thus, when both auxiliary systems are completely synchronized with their original systems for an appropriate coupling strength, then there exists a function that maps systems 1 and 2 to the common (global) GS manifold.

In order to characterize the transition from partial to global GS and to evaluate the stability of the CS of each of the main and auxiliary systems, we have calculated the MTLEs of the main and auxiliary systems which in turn ensure the stability of GS manifold between the original systems. We have also

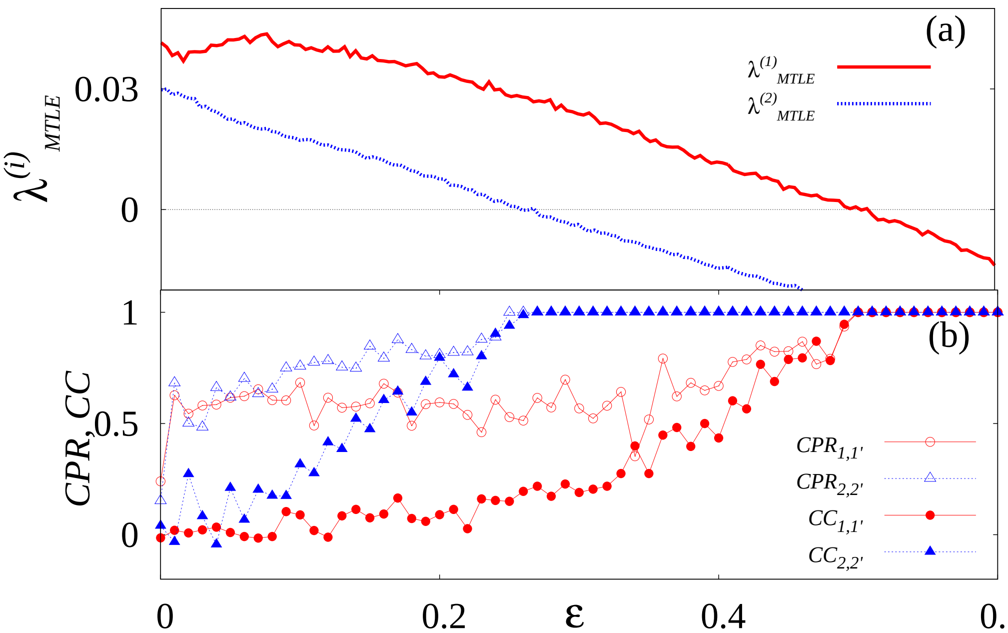

Fig. 4. (a) MTLEs and (b) CC, CPR of the main and auxiliary systems for two mutually coupled MG-PWL systems as a function of $\varepsilon \in (0.0, 0.6)$ for $N = 2$ (13b).

estimated the correlation coefficient (CC) of each of the main and the associated auxiliary systems, given by

$$C_{i,i'} = \frac{\langle (x_i(t) - \langle x_i(t)\rangle)(x'_i(t) - \langle x'_i(t)\rangle)\rangle}{\sqrt{\langle (x_i(t) - \langle x_i(t)\rangle)^2\rangle \langle (x'_i(t) - \langle x'_i(t)\rangle)^2\rangle}}, \tag{14}$$

where the $\langle ... \rangle$ brackets indicate temporal average. If the two systems are in CS state, the correlation coefficient $CC \approx 1$, otherwise $CC < 1$. Further, the existence of PS (between the main and auxiliary systems) can be characterized by the value of the index CPR. If the phases of the coupled systems are mutually locked, then the probability of recurrence is maximal at a time and CPR ≈ 1. In contrast, one can expect a drift in the probability of recurrence resulting in low values of CPR characterizing the degree of locking between the coupled systems [Marwan *et al.*, 2007; Senthilkumar *et al.*, 2006].

The coupled equations (1) and (11) are integrated using the Runge-Kutta fourth order method. The MTLEs are the largest Lyapunov exponents of the evolution equation of $\dot{\Delta}_i \equiv \dot{x}_i - \dot{x}'_i,\ i = 1, 2, 3, 4$. The Lyapunov exponents are calculated using J. D. Farmer's approach [Lakshmanan & Senthilkumar, 2010]. In Fig. 4, we have plotted the various characterizing quantities based on our numerical analysis. The red (light gray) continuous line in Fig. 4(a) shows the MTLE ($\lambda^{(1)}_{MTLE}$) of the MG systems (x_1, x'_1) and the blue (dark gray) dotted line depicts the MTLE ($\lambda^{(2)}_{MTLE}$) of the PWL systems (x_2, x'_2) as a function of the coupling strength. Figure 4(b) shows the CC and CPR of the main and auxiliary MG time-delay systems as red (light gray) filled and open circles, respectively, and the CC and CPR of the PWL systems are represented by the blue (dark gray) filled and open triangles. Initially, for $\varepsilon = 0$, both $CC_{1,1'}$ and $CC_{2,2'}$ are nearly zero, indicating the desynchronized state when both $\lambda^{(1)}_{MTLE}$ and $\lambda^{(2)}_{MTLE} > 0$ which confirm that CS (GS) is unstable. If we increase the coupling strength, $CC_{2,2'}$ and $CPR_{2,2'}$ start to increase towards unity and at $\varepsilon_c^{(2)} \approx 0.26$, $CC_{2,2'} = 1$ ($CPR_{2,2'} = 1$), where $\lambda^{(2)}_{MTLE} < 0$, which confirm the simultaneous existence of GS and PS in the PWL system, while the MG system continues to remain in a desynchronized state ($CC_{2,2'} \approx 0.2$ and $\lambda^{(1)}_{MTLE} > 0$) (partial GS). Further, if we increase the coupling strength to a threshold value $\varepsilon_c^{(1)} \approx 0.5$, a global GS occurs where both $CC_{1,1'}$ and $CC_{2,2'}$ become unity and $\lambda^{(1)}_{MTLE}$ and $\lambda^{(2)}_{MTLE}$ become negative. The transition of the MTLE of the auxiliary and its original systems from positive to

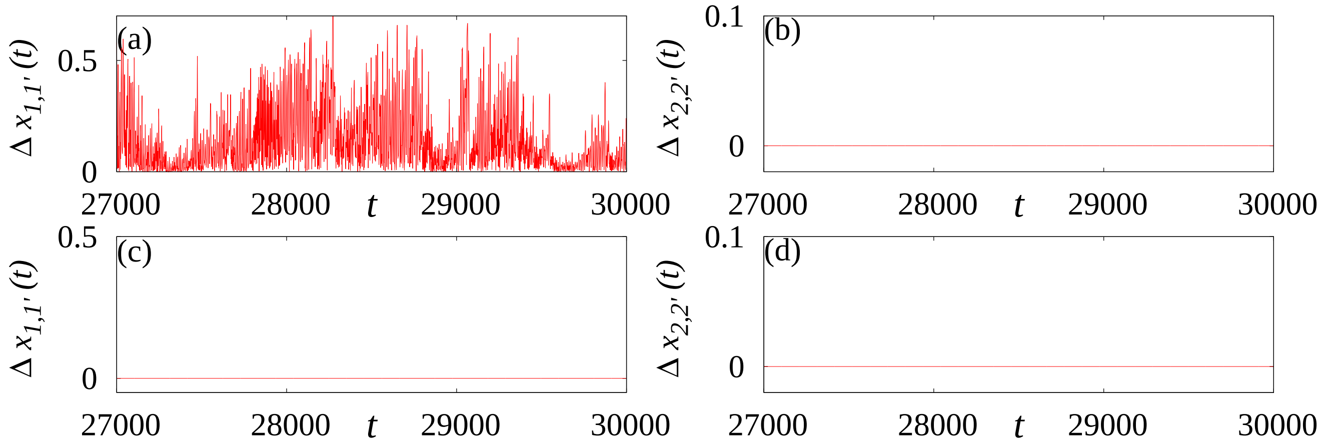

Fig. 5. (a, b) The magnitude of difference in the trajectories between the systems ($\Delta x_{i,i'} = |x_i - x'_i|, \quad i = 1, 2$) for $\varepsilon = 0.3$, and (c, d) for $\varepsilon = 0.55$ for $N = 2$ mutually coupled MG and PWL systems.

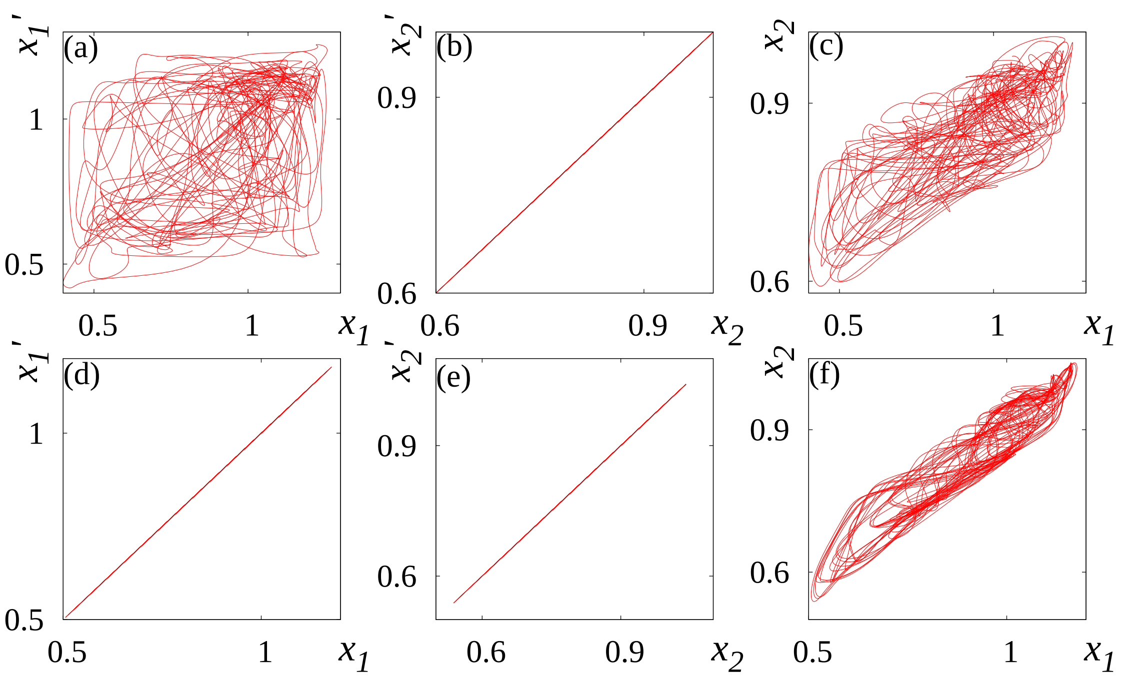

Fig. 6. (a-c) The phase portraits of the systems (x_1, x'_1), (x_2, x'_2) and (x_1, x_2) for $\varepsilon = 0.3$, and (d-f) for $\varepsilon = 0.55$ for $N = 2$.

negative values as a function of the coupling strength strongly confirms the existence of an attracting manifold. To be more clear, for the value of the coupling strengths in range of global GS, a negative value of the MTLE assures the convergence of the perturbed trajectories in the synchronization manifold (CS between the main and auxiliary systems and GS manifold between the main systems). The convergence corroborates the attracting nature of the synchronization manifold. Further, normally one may expect that the systems with lower dynamical complexity will converge to GS manifold first, followed by the system with higher dynamical complexity [Zheng *et al.*, 2002]. But in our studies we encounter a contrary behavior, where the PWL system with three positive LEs reaches the GS manifold first (at $\varepsilon_c^{(2)} \approx 0.26$) and then the MG system (with two positive LEs) converges to the GS manifold at $\varepsilon_c^{(1)} \approx 0.5$ confirming the existence of a transition from partial to global GS in distinctly nonidentical time-delay systems.

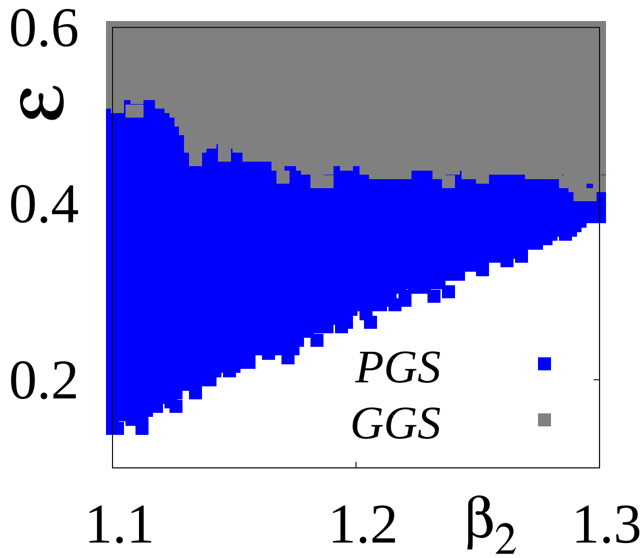

Fig. 7. Phase diagram in the $(\beta_2 - \varepsilon)$ plane for two mutually coupled MG-PWL systems showing partial (blue/dark gray), global (light gray) GS and desynchronization (white) regimes.

We have also numerically computed the synchronization error $(\Delta x_{i,i'}(t) = |x_i(t) - x'_i(t)|, \ \ i = 1, 2)$ and phase projection plots, which are depicted in Figs. 5 and 6, respectively. In the absence of the coupling all the systems evolve with their own dynamics. If we slowly increase the coupling strength the main and the auxiliary PWL systems become completely synchronized for $\varepsilon_c^{(2)} = 0.26$. The synchronization error $\Delta x_{2,2'}(t) = 0$ and the linear relation between the systems (x_2, x'_2) in Fig. 5(b) and in Fig. 6(b) (plotted for $\varepsilon^{(2)} = 0.3$), respectively, confirm that the systems x_2 and x'_2 are in a CS state, whereas the MG systems (x_1, x'_1) remain desynchronized as confirmed by the phase projection [Fig. 6(a)] for the same value of the coupling strength. We also note here that for this value of coupling strength the systems x_1 and x_2 show certain degree of correlation as depicted in Fig. 6(c). If we increase ε further, the systems (x_1, x'_1) and (x_2, x'_2) reach the CS manifold (for $\varepsilon_c^{(1)} = 0.5$) and one may expect that both x_1 and x_2 attain the common GS manifold, which we call as global GS. Both synchronization errors $\Delta x_{1,1'}(t)$ and $\Delta x_{2,2'}(t)$ become zero as shown in Figs. 5(c) and 5(d) for $\varepsilon_c^{(1)} = 0.55$. This fact confirms the existence of a global GS state. Further, Figs. 6(d) and 6(e) show a linear relation between the systems (x_1, x'_1) and (x_2, x'_2), respectively, which additionally confirms the existence of global GS. The degree of correlation in the phase space between the systems x_1 and x_2 for the global GS state is depicted in Fig. 6(f) for the same value of coupling strength.

To obtain a global picture on the occurrence of transition from partial to global GS between the MG and PWL systems, we have plotted the values of $CC_{i,i'}$ as a 2-parameter diagram in the $(\beta_2 - \varepsilon)$ plane. We have fixed the parameter values of the MG systems (as given in Sec. 2) and vary one of the parameter $(\beta_2 \in (1.1, 1.3))$ of the PWL system as a function of the coupling strength $(\varepsilon \in (0.1, 0.6))$ as depicted in Fig. 7. The white region indicates the desynchronized state and the blue (dark gray) region corresponds to the partial GS region, where only one of the mutually coupled systems has reached the common GS manifold as indicated by the unit value of the $CC_{i,i'}$. The global GS is represented by light gray where both coupled systems are in GS manifold as confirmed by the unit value of $CC_{i,i'}$ of both systems.

We have also analytically investigated the existence of the transition from partial to global GS using the Krasovskii-Lyapunov functional theory. In this connection, we consider the difference between the state variables (synchronization error) of the main and the associated auxiliary systems $(\Delta_i = x_i - x'_i, \ \ i = 1, 2)$. For small values of Δ_i, the evolution equation for the CS manifold of the MG systems $(\Delta_1 = x_1 - x'_1)$ can be written as

$$\dot{\Delta}_1 = -(\alpha_1 + \varepsilon)\Delta_1 + \beta_1[f_1'(x_{\tau_1})]\Delta_{1\tau_1} \tag{15}$$

where $x_{\tau_1} = x(t - \tau_1)$ and $\Delta_{1\tau_1} = \Delta_1(t - \tau_1)$. The CS manifold is locally attracting if the origin of Eq. (15) is stable. From the Krasovskii-Lyapunov theory, a continuous positive definite Lyapunov functional can be defined as

$$V(t) = \frac{1}{2}\Delta_1^2 + \mu \int_{-\tau}^{0} \Delta_1^2(t + \theta)d\theta, \qquad V(0) = 0, \tag{16}$$

where $\mu > 0$ is an arbitrary positive parameter. The Lyapunov function $V(t)$ approaches zero as $\Delta_1 \to 0$. The derivative of the above equation (16) can be written as

$$\frac{dV}{dt} = -[\alpha_1 + \varepsilon]\Delta_1^2 + \beta_1[f_1'(x_{\tau_1})]\Delta_1\Delta_{1\tau_1} + \mu\Delta_1^2 - \mu\Delta_{1\tau_1}^2, \tag{17}$$

which should be negative for stability of the CS manifold, that is $\Delta_1 = 0$. This requirement results in a condition for stability as

$$(\alpha_1 + \varepsilon) > |\beta_1 f_1'(x_{\tau_1})|. \tag{18}$$

From Eq. (18), one can see that the stability condition depends on the nonlinear function $f(x)$ of the individual systems. Hence from the form of the nonlinear function of the MG system [Eq. (2)], we have

$$f_1'(x_{\tau_1}) = \frac{(1 + x_{\tau_1}^c) - cx_{\tau_1}^c}{(1 + x_{\tau_1}^c)^2}. \tag{19}$$

Consequently, the stability condition becomes,

$$(\alpha_1 + \varepsilon) > \left|\beta_1\left(\frac{(1 + x_{\tau_1}^c) - cx_{\tau_1}^c}{(1 + x_{\tau_1}^c)^2}\right)\right|. \tag{20}$$

It is not possible to find the exact value of the nonlinear function $f'(x_\tau)$ as it depends on the value of the variable x_{τ_1}. However, it is possible to find the value of $f_1'(x_{max})$ by identifying the maximal value of x_{max} using the Lyapunov-Razumikin function (which is a special class of the Krasovskii-Lyapunov theory). From the hyperchaotic attractor of the MG system, for the chosen parameter values, one can identify the maximum value of $x_{max} = 1.24$. So the stability condition becomes $\varepsilon > |\beta_1 f_1'(x_{max\ \tau_1})| - \alpha \approx 0.33$ (a sufficient condition for the global GS). From Fig. 4, the threshold value of the coupling strength to attain GS in the MG systems is $\varepsilon_c^{(1)} \approx 0.5$ (> 0.33) for which the stability condition is satisfied.

Now, one can find the evolution equation for the CS manifold corresponding to the PWL time-delay system $(x_2 - x_2')$ as $\dot{\Delta}_2 = -(\alpha_2 + \varepsilon)\Delta_2 + \beta_2[f_2'(x_{\tau_2})]\Delta_{2\tau_2}$ and with a similar procedure as above, the stability condition for the PWL systems becomes $(\alpha_2 + \varepsilon) > |\beta_2 f_2'(x_{\tau_2})|$. Now from the form of the piecewise linear function $f_2(x)$ in Eq. (3), we have

$$f_2'(x_{\tau_2}) = \begin{cases} 1.5, & 0.8 \leq |x| \leq \frac{4}{3} \\ 1.0, & |x| < 0.8 \end{cases} \tag{21}$$

Consequently, the stability condition becomes $(\alpha_2 + \varepsilon) > |\beta_2|$, corresponding to the inner regime of the nonlinear function where most of the system dynamics is confined for the asymptotic CS state $\Delta_2 = 0$. From Fig. 4, one can find that CS between the PWL systems occurs for a coupling strength $\varepsilon_c^{(2)} > 0.27$, satisfying the sufficient stability condition for partial GS, $\varepsilon > |\beta_2| - \alpha_2 = 0.2$ $(0.27 > 0.2)$.

4. Detection of Global GS Using the Mutual False Nearest Neighbor Method

Next, we use the mutual false nearest neighbor method to confirm the existence of global GS in distinctly different time-delay systems. The main idea of this technique consists of the fact of preserving the local neighborliness between the states of the interacting systems [Rulkov *et al.*, 1995]. Let us consider the trajectories of two systems which are connected by the relation $y(t) = \phi(x(t))$ (condition for GS). The MFNN method depends on the observation that in GS state two neighboring points in the phase space of

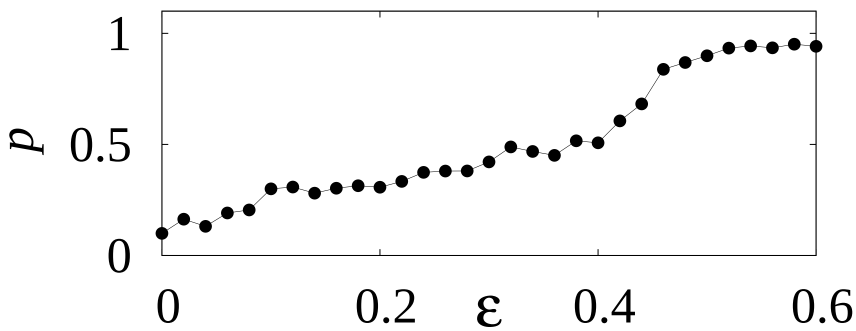

Fig. 8. MFNN parameter (p) as a function of coupling strength (ε) showing global GS state for $N = 2$ mutually coupled MG-PWL time-delay systems (corresponding to Fig. 4).

the drive system $x(t)$ correspond to two neighboring points in the phase space of the response system $y(t)$. For mutually coupled systems, the inverse statement is also valid. That is, all close states in the phase space of the system $y(t)$ must correspond to close states of the system $x(t)$.

Let us consider a set of embedded vector points (obtained by attractor reconstruction using time-delay embedding methods [Abarbanel *et al.*, 1993; Packard *et al.*, 1980]) in the spaces of the drive $(X_1, X_2, \cdots)$ and response $(Y_1, Y_2, \cdots)$ systems coming from finite segments of the trajectories sampled at uniform intervals of time. Now we can choose an arbitrary point X_n in the phase space of the drive system. Let the nearest phase space neighbor of this point in the reconstructed attractor be X_{nNND}. In GS state, one can also expect that the corresponding points of the response system Y_n will have Y_{nNND} as its close neighbor. From the GS relation, the distance between the two nearest neighbors in the phase space of the response system can be written as $Y_n - Y_{nNND} = D\phi(X_n)(X_n - X_{nNND})$, where $D\phi(X_n)$ is the Jacobian matrix of the transformation ϕ evaluated at X_n. Similarly, we consider the point Y_n and locate its nearest neighbor from the time series as Y_{nNND}. Again using the GS relation, the distance between the points of the response variables can be written as $Y_n - Y_{nNNR} = D\phi(X_n)(X_n - X_{nNNR})$. This suggests that the ratio for the MFNN parameter can be written as,

$$p = \frac{1}{T}\sum_{n} \frac{|Y_n - Y_{nNND}|}{|X_n - X_{nNND}|} \frac{|X_n - X_{nNNR}|}{|Y_n - Y_{nNNR}|}, \tag{22}$$

where T is the sampling time. In GS state the MFNN parameter (p) will be of the order of unity. This method has been widely used to identify GS in mutually coupled systems.

The MFNN parameter (p) for two mutually coupled MG and PWL time-delay systems is depicted in Fig. 8 (corresponding to Fig. 4). As can be seen from this figure the value of p becomes close to unity above $\varepsilon > 0.5$, which is indeed the critical coupling strength $\varepsilon_c^{(1)}$ in Fig. 4, strongly confirming the existence of global GS.

5. Transition from Partial to Global GS in $N = 3$ Mutually Coupled Time-delay Systems

Now, we extend the above analysis to $N = 3$ mutually coupled distinctly nonidentical systems in an array and a ring configuration [Figs. 3(b) and 3(c)]. In addition to the above two time-delay systems, now we have considered the third system as TPWL with the nonlinear function $f_3(x)$ as given in Eq. (4). The system parameters are fixed as in Sec. 2. For this chosen set of parameter values the system exhibits a hyperchaotic attractor (Fig. 1(c)) with four positive LEs ($D_{KY} = 8.211$) [see Fig. 2(c)].

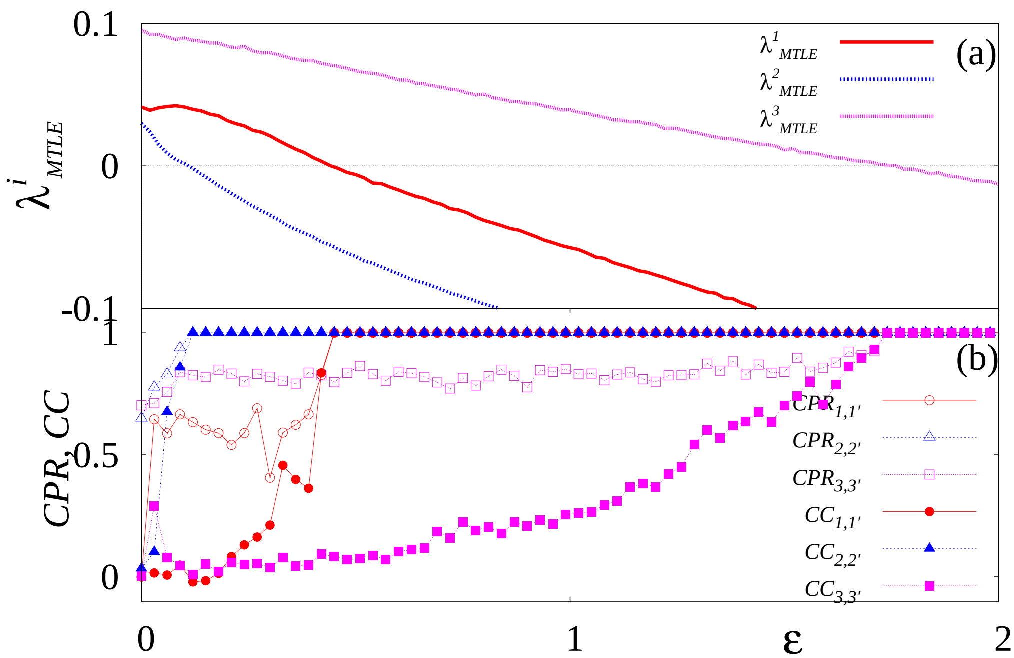

Fig. 9. (a) MTLEs and (b) CC, CPR of the main and auxiliary systems for $N = 3$ distinctly nonidentical time-delay systems with an linear array configuration as a function of ε.

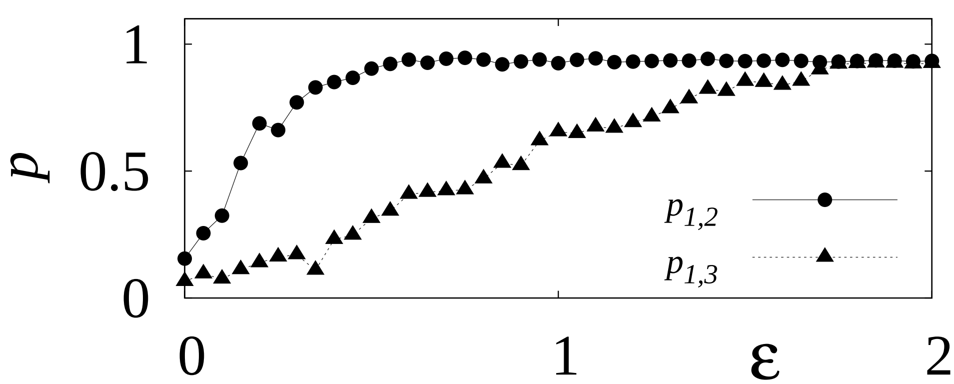

Fig. 10. MFNN parameter (p) for the linear array of $N = 3$ mutually coupled time-delay systems as a function of the coupling strength shows the global GS state (corresponding to Fig. 9). See text for details.

5.1. *Three mutually coupled systems with array configuration*

First, we illustrate the transition from partial to global GS in a linear array of $N = 3$ mutually coupled systems using the auxiliary system approach. The schematic diagram for this configuration is given in Fig. 3(b). Here the systems 1, 2 and 3 are mutually coupled with their neighboring systems as depicted in Fig.3(b) and the associated auxiliary systems are driven by the neighboring main systems. For example, x'_1 is driven by x_2, while x'_2 by x_1 and x_3, and x'_3 by x_2. MTLEs, CC and CPR of all the three main and auxiliary systems are shown in Fig. 9(a) and 9(b) as a function of the coupling strength. In the absence of the coupling ($\varepsilon = 0$), positive values of MTLEs ($\lambda^{(i)}_{MTLE} > 0$) and the low values of $CC_{i,i'}$ and $CPR_{i,i'}$ indicate that the main and the corresponding auxiliary systems evolve independently. Increasing the coupling strength from null value results in decreasing $\lambda^{(i)}_{MTLE}$ and increasing $CC_{i,i'}$ and $CPR_{i,i'}$.

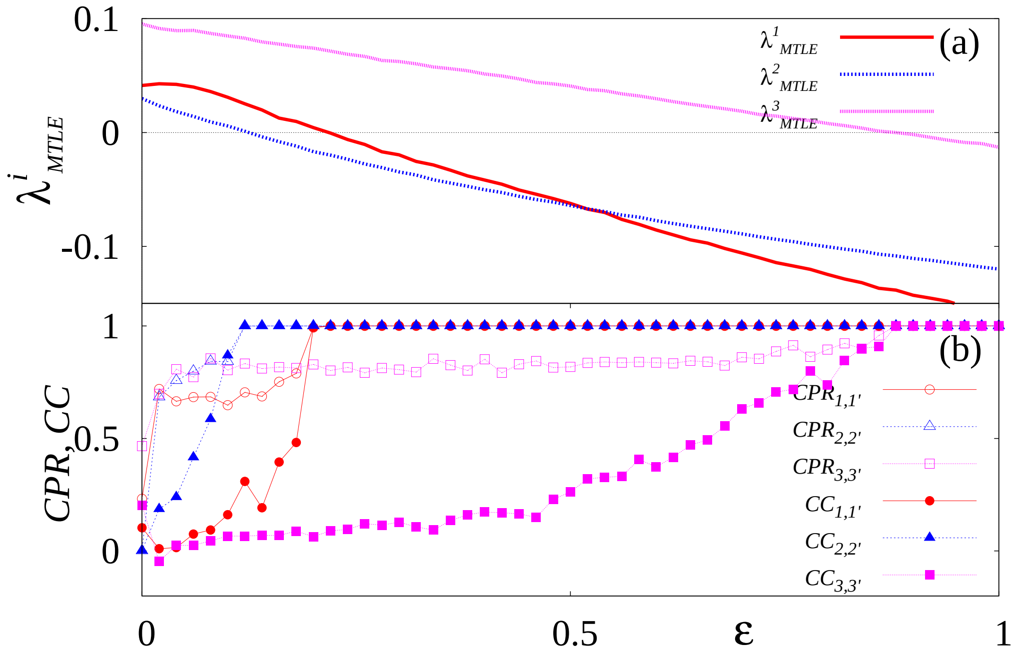

Fig. 11. (a) MTLEs and (b) CC, CPR of the main and auxiliary systems for $N = 3$ distinctly nonidentical time-delay systems with ring configuration as a function of ε.

If we increase the coupling strength to $\varepsilon_c^{(2)} = 0.12$, the PWL systems with three positive LEs becomes synchronized first as evidenced by $\lambda^{(2)}_{MTLE} < 0$, $CC_{2,2'} = 1$ and $CPR_{2,2'} = 1$, indicating the onset of partial GS. The MTLE of the MG systems with two positive LEs becomes negative ($\lambda^{(1)}_{MTLE} < 0$) along with $CC_{1,1'} = 1$ and $CPR_{1,1'} = 1$ at $\varepsilon_c^{(1)} = 0.45$ which confirms that the MG system reaches the common GS manifold, while the TPWL systems are not yet synchronized. Finally for $\varepsilon_c^{(3)} = 1.74$, the TPWL system with four positive LEs attains the CS state with $\lambda^{(3)}_{MTLE} < 0$ and $CC_{3,3'}$ and $CPR_{3,3'}$ reaching unit values exactly at the same threshold value of the coupling strength ($\varepsilon_c^{(3)}$) indicating the existence of global GS. This also confirms the simultaneous existence of GS and PS in an array of three mutually coupled systems.

For $N > 2$, it is not possible to obtain accurate analytical results for all the coupled systems with respect to the numerical simulation results due to the complexity in the coupling architecture. We have also calculated the MFNN parameter (p) for the linear array of three mutually coupled time-delay systems as a function of the coupling strength, which is depicted in Fig. 10 (corresponding to Fig. 9). The MFNN parameter for the MG and PWL systems (systems 1 and 2) becomes close to unity at $\varepsilon > 0.45$ (filled circle). The MFNN parameter p of the MG and TPWL systems (systems 1 and 3) approximately reaches the unit value at $\varepsilon > 1.74$ (filled triangle) agreeing perfectly with the threshold values indicated by MTLEs, CC and CPR, all confirming the existence of global GS in the array.

5.2. *Three mutually coupled systems with ring configuration*

Next, we consider a system of three mutually coupled systems with a ring configuration along with their corresponding auxiliary systems (here each auxiliary system is driven by the other two systems, for example, x_1' is driven by x_2 and x_3, x_2' by x_1 and x_3 and x_3' by x_1 and x_2, as depicted in the schematic diagram Fig. 3(c)). CC, CPR and MTLEs for the mutually coupled ring of the above three distinctly nonidentical systems are shown in Fig. 11(a) and 11(b). Again all the three systems (PWL, MG and TPWL) reach their CS (GS) manifold for the threshold values $\varepsilon_c^{(i)} \approx 0.12, 0.22$ and $0.88, i = 1, 2, 3$, respectively, as indicated by

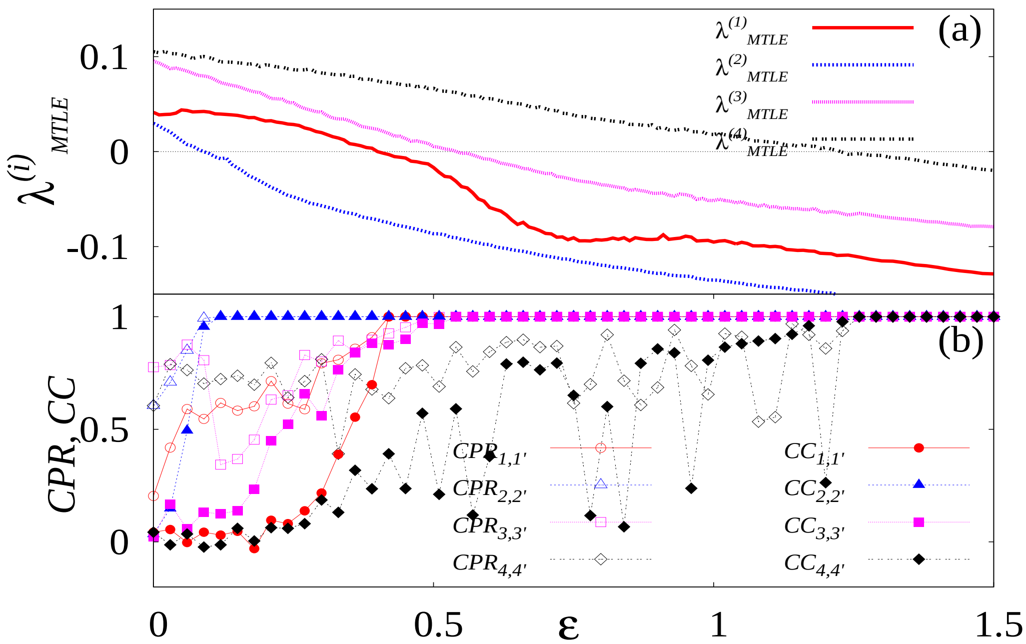

Fig. 12. (a) MTLEs and (b) CC, CPR of the main and auxiliary systems for $N = 4$ distinctly nonidentical time-delay systems with linear array configuration as a function of ε.

the transition of their $\lambda^{(i)}_{MTLE}$ below zero [Fig. 11(a)]. In addition all $CC_{i,i'}$ and $CPR_{i,i'}$ reach unit values [Fig. 11(b)] exactly at the same threshold values of the coupling strength indicating the simultaneous existence of GS and PS in a ring of three mutually coupled time-delay systems.

It has been already known that structurally different time-delay systems will produce chaotic/hyperchaotic attractors with dissimilar phase space geometry characterized by multiple time-scales (see Fig. 1 for example). In order to preserve the local neighboring points of each of the attractor we have reconstructed the attractors of different time-delay systems with almost identical time-scales. Due to the increased complexity of the topological properties of chaotic/hyperchaotic attractors of the network of ring, global and star configurations, it is not possible to obtain the reconstructed attractor with similar time-scales in structurally different time-delay systems and hence MFNN cannot be estimated in these cases.

6. Transition from Partial to Global GS in $N = 4$ Mutually Coupled Time-delay Systems

In this section, we demonstrate the existence of transition from partial to global GS in four (only in $N = 4$ for clear visibility of figures depicting synchronization transitions) mutually coupled distinctly nonidentical time-delay systems in the following configurations: a ring, an array, a global and a star. In addition to the above three time-delay systems discussed in the previous sections, as a fourth system, we consider the Ikeda time-delay system with the nonlinear function as in Eq. (6) [Ikeda *et al.*, 1980]. This system exhibits a hyperchaotic attractor [Fig. 1(d)] with five positive LEs [Fig. 2(d)] with a KY dimension $K_{DY} = 10.116$ for the chosen parameter values.

6.1. *Four mutually coupled systems with an array configuration*

First we demonstrate the existence of transition from partial to global GS in four mutually coupled time-delay systems (MG, PWL, TPWL and Ikeda) in a linear array configuration. The schematic diagram for this configuration is depicted in Fig. 3(d). In Figs. 12(a) and 12(b), we have again presented the characterizing

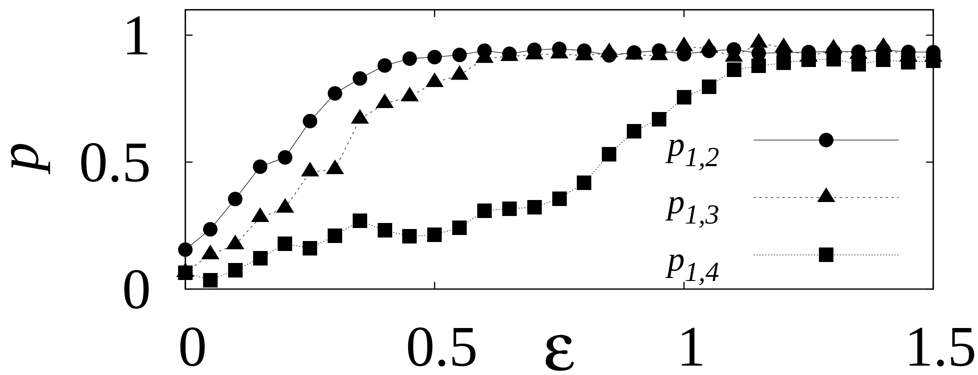

Fig. 13. MFNN parameter (p) for the linear array of mutually coupled systems with $N = 4$ as a function of the coupling strength showing the global GS state (corresponding to Fig. 12).

quantities $\lambda^{(i)}_{MTLE}$, $CC_{i,i'}$ and $CPR_{i,i'}, i, i' = 1, 2, 3, 4$ of all the four systems along with their associated auxiliary systems as a function of coupling strength. For $\varepsilon = 0$, $\lambda^{(i)}_{MTLE} > 0$, while $CC_{i,i'}$ and $CPR_{i,i'}$ show low values corresponding to a desynchronized state. At $\varepsilon^{(2)}_c = 0.09$ and $\varepsilon^{(1)}_c = 0.4$, $\lambda^{(2)}_{MTLE}$ of the PWL systems and $\lambda^{(1)}_{MTLE}$ of the MG systems become negative, respectively, which confirm that these systems reach the CS (GS) state with their corresponding auxiliary (main) systems, whereas the other two systems are not yet synchronized ($\lambda^{(3,4)}_{MTLE} > 0$). Increasing the coupling strength, we find that at $\varepsilon^{(4)}_c = 0.54$ the Ikeda systems with five positive LEs attain the CS (GS) manifold when $\lambda^{(4)}_{MTLE} < 0$ and finally the TPWL system becomes synchronized at $\varepsilon^{(3)}_c = 1.2$, confirming the transition from partial to global GS in four mutually coupled time-delay systems in an array configuration. The $CC_{i,i'}$ and $CPR_{i,i'}$ of the corresponding systems show a clear transition to unit value for their corresponding threshold values of $\varepsilon^{(i)}_c$ confirming the simultaneous existence of GS and PS [Fig. 12(b)]. We have again calculated the MFNN parameter (p) for $N = 4$ mutually coupled linear array of time-delay systems by taking the MG time-delay system as a reference system as depicted in Fig. 13. The unit value of the MFNN parameter p of the respective $\varepsilon^{(i)}_c$ values of PWL, TPWL and Ikeda time-delay systems (with respect to the MG time-delay system) confirms the existence of the transition from partial to global GS .

6.2. *Four mutually coupled systems with a ring configuration*

Next, we illustrate the existence of a transition from partial to global GS in a ring of $N = 4$ mutually coupled distinctly nonidentical time-delay systems [Fig. 3(e)]. MTLEs, CC and CPR of all the four main and corresponding auxiliary systems are depicted in Figs. 14(a) and 14(b). In the absence of the coupling, all the systems evolve independently as evidenced by the fact that $\lambda^{(i)}_{MTLE} > 0, i = 1, 2, 3, 4$, and low values of $CC_{i,i'}$ and $CPR_{i,i'}$. The transitions of MTLEs ($\lambda^{(i)}_{MTLE} < 0$) from positive to negative values of the MG, PWL, TPWL and Ikeda systems indicate that they reach their CS (GS) manifolds for the threshold values of the coupling strengths $\varepsilon^{(i)}_c = 0.092,\ 0.088,\ 0.75$ and 0.65, respectively. Further, GS and PS also occur simultaneously as indicated by the $CC_{i,i'}$ and $CPR_{i,i'}$ [in Fig. 14(b)] of the systems in the ring configuration.

6.3. *Four mutually coupled systems with global and star configurations*

In this section, we study the transition from partial to global GS in global (all-to-all) and star coupling configurations with $N = 4$ time-delay systems with different fractal dimensions. The schematic diagrams of the global and star coupling configurations are depicted in Figs. 3(f) and 3(g), respectively. MTLEs,

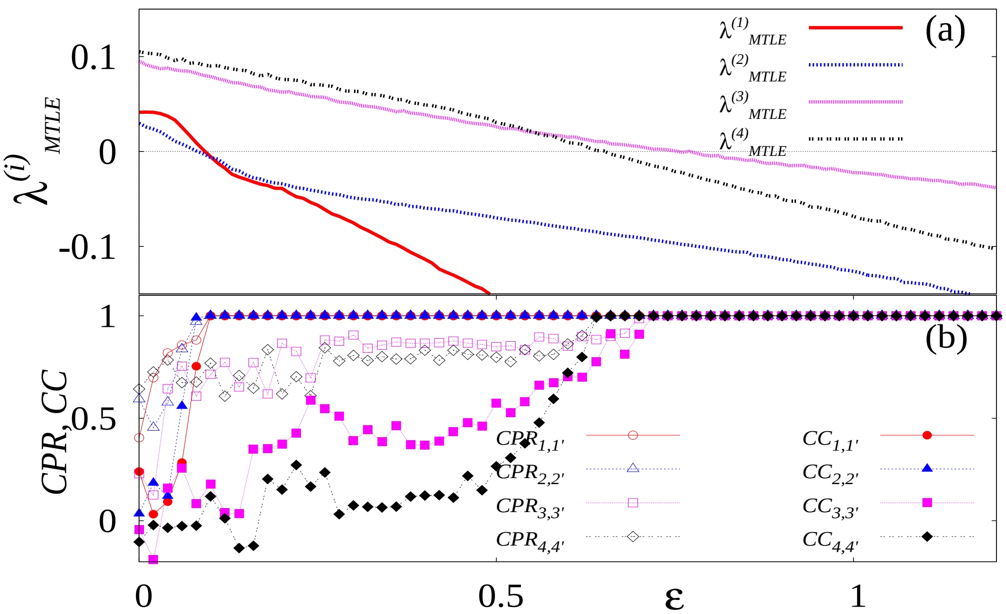

Fig. 14. (a) MTLEs and (b) CC, CPR of the main and auxiliary systems for $N = 4$ distinctly nonidentical time-delay systems with ring configuration as a function of ε.

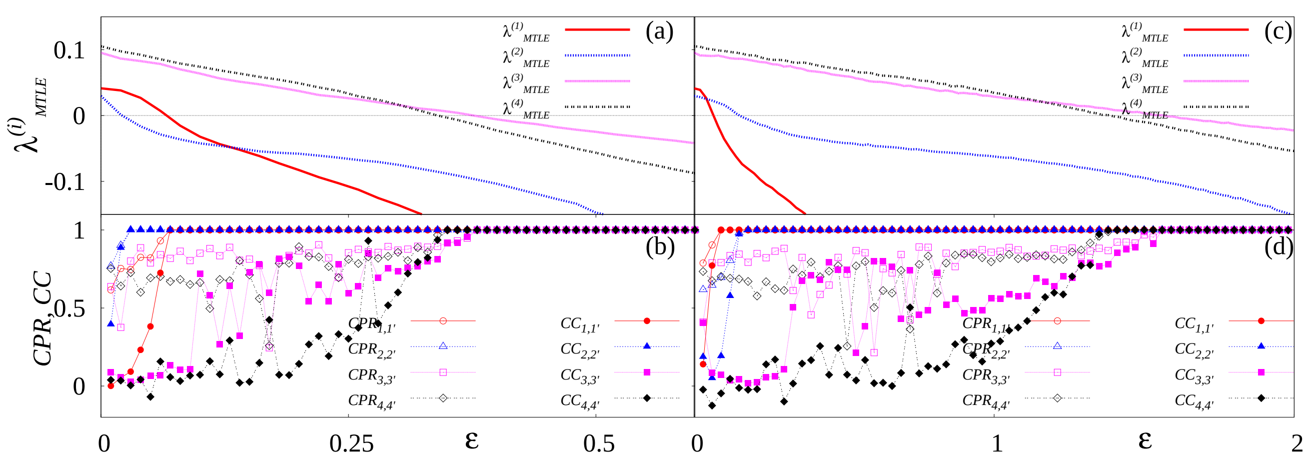

Fig. 15. (a) MTLEs and (b) CC, CPR of the main and auxiliary systems of four distinctly nonidentical time-delay systems with global coupling as a function of ε. (c) and (d) are the corresponding figures for star configuration.

CC and CPR of all the four systems are depicted in Figs. 15(a-b) and 15(c-d) for global and star coupling configurations, respectively. In the case of global coupling configuration, $\lambda^{(2)}_{MTLE}$ of the PWL systems and $\lambda^{(1)}_{MTLE}$ of the MG systems become negative at $\varepsilon^{(2)}_c = 0.03$ and $\varepsilon^{(1)}_c = 0.07$, respectively, while the other two systems evolve independently. When the coupling strength is increased to $\varepsilon^{(4)}_c = 0.35$, the Ikeda system gets synchronized ($\lambda^{(4)}_{MTLE} < 0$) and finally $\lambda^{(3)}_{MTLE}$ of the TPWL system becomes negative at $\varepsilon^{(3)}_c = 0.38$, thereby confirming the onset of a global GS state in globally coupled network of distinctly nonidentical time-delay systems. Further, the values of $CC_{i,i'}$ and $CPR_{i,i'}$ reach unit value at the same values of the coupling strength as above indicating the simultaneous occurrence of GS and PS [Fig. 15(b)].

In the star configuration, $\lambda^{(2)}_{MTLE}$ transits first from positive to negative values at $\varepsilon^{(2)}_c = 0.09$ showing a

CS between PWL and its auxiliary system [Fig. 15]. This is followed by the value of $\lambda^{(1)}_{MTLE}$ of MG systems becoming negative at $\varepsilon_c^{(1)} = 0.18$. Next for the Ikeda systems $\lambda^{(4)}_{MTLE}$ becomes negative at $\varepsilon_c^{(4)} = 1.4$ and finally the $\lambda^{(3)}_{MTLE}$ of TPWL systems becomes negative at $\varepsilon_c^{(3)} = 1.56$, confirming the existence of global GS. Further, for the same values of coupling strength, $CC_{i,i'}$ and $CPR_{i,i'}$ reach unit values confirming the simultaneous occurrence of GS and PS in four distinctly nonidentical coupled time-delay systems with different fractal dimensions.

In addition, we have also confirmed that there exist a similar type of synchronization transitions in other permutations on the order of the systems between MG, PWL, TPWL and Ikeda systems in all coupling configurations.

7. Transition from Partial to Global GS in Time-delay Systems of Different Orders

Now, we will demonstrate the genericity of the transition from partial to global GS by revealing it in coupled time-delay systems of different orders so as to prove that the reported phenomenon is not restricted to time-delay equations with structural similarity alone. In particular, we will show the existence of a transition to global GS via partial GS in such systems using the measures CC and CPR. Mutual coupling is introduced in the x variable of higher order systems. We will demonstrate the above results in the following coupled systems.

(1) In a system consisting of a mutually coupled Ikeda time-delay system (which is a scalar first order time-delay system) and a Hopfield neural network [Hopfield, 1998; Meng & Wang, 2007; Lakshmanan & Senthilkumar, 2010] (which is a second order time-delay system), and
(2) In a system of mutually coupled MG time-delay system (which is a scalar first order time-delay system) and a plankton model [Abraham, 1998; Gakkhar & Singh, 2010] (which correspond to a third order system with multiple delays),

A class of delayed chaotic neural networks [Hopfield, 1998; Meng & Wang, 2007; Lakshmanan & Senthilkumar, 2010] can be represented as a set of coupled DDEs as given by the equation

$$\dot{x}(t) = -Cx(t) + Af\left[x(t)\right] + Bf\left[x(t-\tau)\right], \tag{23}$$

where $x(t) = [x_1(t), x_2(t), \cdots, x_n(t)]^T \in R^n$ is the state vector, the activation function $f\left[x(t)\right] = \left(f_1\left[x_1(t)\right], f_2\left[x_2(t)\right], \cdots, f_n\left[x_n(t)\right]\right)^T$ denotes the manner in which the neurons respond to each other. C is a positive diagonal matrix, $A = (a_{ij}), i, j = 1, 2, \cdots, n$ is the feedback matrix, $B = (b_{ij})$ represents the delayed feedback matrix with a constant delay τ. The general class of delayed neural networks represented by the above Eq. (23) unifies several well known neural networks such as the Hopfield neural networks and cellular neural networks with delay.

The specific set of delayed neural networks (Eq. (23)) which corresponds to the Hopfield neural networks is for the choice of the activation function

$$f\left[x(t)\right] = \tanh\left[x(t)\right], \tag{24}$$

and for the value of the matrices

$$C = \begin{bmatrix} 1 & 0 \\ 0 & 1 \end{bmatrix}, \quad A = \begin{bmatrix} 2.0 & -0.1 \\ -5.0 & 3.0 \end{bmatrix}, \quad B = \begin{bmatrix} -1.5 & -0.1 \\ -0.2 & -2.5 \end{bmatrix}.$$

Next, we will illustrate the existence of global GS via partial GS in a system of mutually coupled Ikeda time-delay systems and the Hopfield neural network. The CC and CPR between the main and auxiliary systems are depicted in Fig. 16. Low values of CC and CPR in the absence of coupling indicates the asynchronous behavior of both the systems. Upon increasing the coupling strength from zero, the second order system, that is the Hopfield neural network, reaches the common synchronization manifold first (partial GS) at the threshold value of $\varepsilon_c^{(2)} \approx 0.05$ as indicated by the unit value of the cross correlation

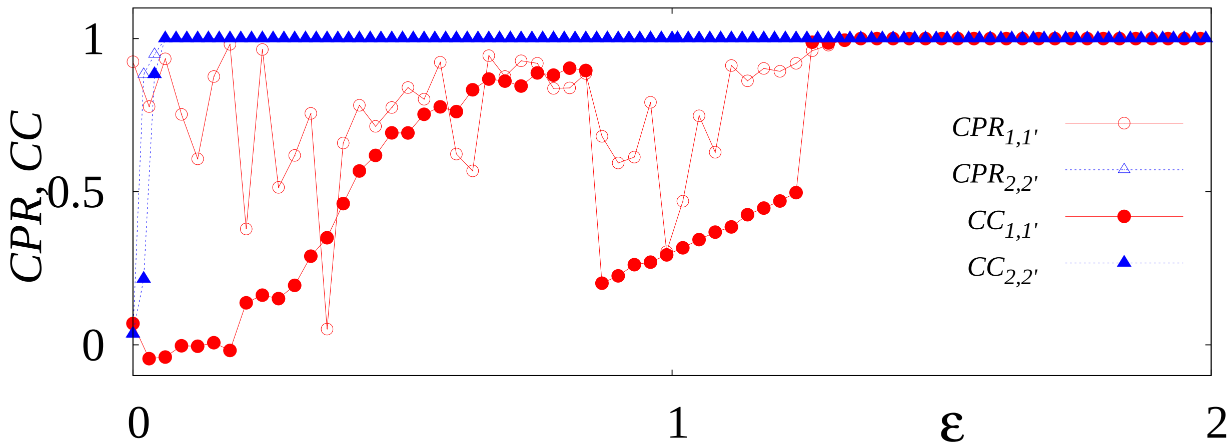

Fig. 16. CC and CPR of the main and auxiliary systems of a coupled Ikeda time-delay system and Hopfield neural network.

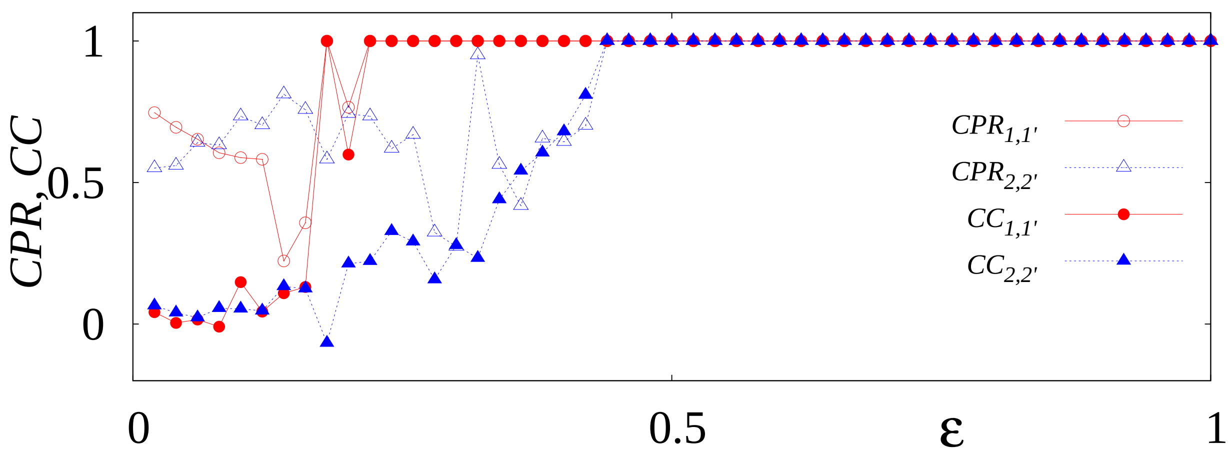

Fig. 17. CC and CPR of the main and auxiliary systems of a coupled Mackey-Glass time-delay system and the plankton model (25c).

coefficient $CC_{2,2'}$, while the Ikeda system remains in its transition state. The simultaneous existence of phase synchronization (PS) together with GS is also confirmed by the unit value of $CPR_{2,2'}$ at the same $\varepsilon_c^{(2)}$. Further increase in the coupling strength results in the synchronization (both GS and PS) of the Ikeda system to the common synchronization manifold for $\varepsilon_c^{(1)} \approx 1.32$ as evidenced from the unit value of $CC_{1,1'}$ and $CPR_{1,1'}$ (Fig. 16) confirming the existence of global GS via partial GS in coupled systems of different orders.

Next, we illustrate the transition from partial to global GS in mutually coupled MG time-delay system, and a third order plankton model [Abraham, 1998; Gakkhar & Singh, 2010] with multiple delays. The normalized system of equations of a zoo-plankton model is represented as

$$\dot{x} = ax[1 - (x + y)] - xy - l_1 xz, \tag{25a}$$

$$\dot{y} = xy - b_2 y - l_2 yz, \tag{25b}$$

$$\dot{z} = -b_1 z + l_1 x(t - \tau_1) z(t - \tau_3) + l_2 y(t - \tau_2) z(t - \tau_3) - n(x + y)z, \tag{25c}$$

where $a = 15.0, b_1 = 1.0, b_2 = 0.2, l_1 = 9.0, l_2 = 13.5$ and $n = 2.0$ are constants. Delays τ_1, τ_2 and τ_3 are in general different may also be different, but for simplicity we have considered identical delays,

$\tau_1 = \tau_2 = \tau_3 = 5.0$, as studied in ref [Gakkhar & Singh, 2010]. Here x, y and z are the normalized quantities of the density of the susceptible phytoplankton, infected phytoplankton and zooplankton (predator species), respectively. Low values of the CC and CPR for $\varepsilon = 0$ between the main and auxiliary systems as shown in Fig. 17 confirm that the systems evolve independently in the absence of coupling between them. As the coupling strength is increased the plankton model synchronizes first to the common synchronization manifold at $\varepsilon_c^{(1)} \approx 0.21$ as denoted by $CC_{1,1'} = 1.0$ indicating partial GS (Fig. 17). PS has also occurred simultaneously at the same threshold value of $\varepsilon_c^{(1)}$ as indicated by the unit value of $CPR_{1,1'}$. Further increase in ε leads to the existence of global GS by synchronizing the MG time-delay system to the common synchronization manifold as both $CC_{2,2'}$ and $CPR_{2,2'}$ attain unity at $\varepsilon_c^{(2)} \approx 0.44$.

Thus, we prove that the transition from partial to global GS phenomenon is not restricted to first order structurally similar systems alone but it is also valid for systems with different orders.

8. Conclusion

In conclusion, we have pointed out the existence of a synchronization transition from partial to global GS in distinctly nonidentical time-delay systems with different fractal dimensions in symmetrically coupled (regular) networks with a linear array, and also in ring, global and star configurations using the auxiliary system approach and the mutual false nearest neighbor method. We have shown that there exists a smooth transformation function even for networks of structurally different time-delay systems with different fractal dimensions, which maps them to a common GS manifold. We have also found that GS and PS occur simultaneously in structurally different time-delay systems. We have calculated MTLEs to evaluate the asymptotic stability of the CS manifold of each of the main and the corresponding auxiliary systems. This in turn, ensures the stability of the GS manifold between the main systems. In addition, we have also estimated the CC and the CPR to characterize the relation between GS and PS. Further, to prove the genericity of our results, we have also demonstrated the synchronization transition in systems with different orders such as coupled MG and the Hopfield neural network model and a system of coupled Ikeda and plankton models. The analytical stability condition for partial and global GS is deduced using the Krasovskii-Lyapuov theory. We wish to note that now we are working on the experimental realization of the existence of partial and global GS in distinctly nonidentical time-delay systems using nonlinear time-delayed electronic circuits.

Acknowledgments

D. V. Senthilkumar acknowledges the supoport from SERB-DST Fast Track scheme for Young Scientists. M. Lakshmanan(M. L.) has been supported by the DST, Government of India sponsored IRHPA research project. M. L. has also been supported by a DST Ramanna Fellowship project and a DAE Raja Ramanna Fellowship.

References

Abarbanel, H. D. I., Rulkov, N. F. & Sushchik, M. M. [1996] "Generalized synchronization of chaos: The auxiliary system approach" *Phys. Rev. E* **53**, 4528.

Abarbanel, H. D. I., Brown, R., Sidorowich, J. J. & Tsimring, L. S. [1993] "The analysis of observed chaotic data in physical systems" *Rev. Mod. Phys.* **65**, 1331.

Abraham, E. R. [1998] "The generation of plankton patchiness by turbulent stirring" *nature* **391**, 577.

Acharyya, S. & Amritkar, R. E. [2013] "Generalized synchronization of coupled chaotic systems" *Eur. Phys. J. Special Topics* **222**, 939.

Amritkar, R. E. & Rajgarajan, G. [2006] "Spatially synchronous extinction of species under external forcing" *Phys. Rev. Lett.* **96**, 258102.

Appeltant, L., Soriano, M. C., Van der. Sande, G., Danckaert, J., Masser, S., Dambre, J., Schrauwen, S., Mirasso, C. R. & Fischer, I. [2011] "Information processing using a single dynamical node as complex system" *Nature Communications* **2**, 468.

Blasius, B., Huppert, A. & Stone, L. [1999] "Complex dynamics and phase synchronization in spatially extended ecological systems" *Nature (London)* **392**, 239.

Boccaletti, S., Valladares, D. L., Kurths, J., Maza, D. & mancini, H. [2000] "Synchronization of chaotic structurally nonequivalent systems" *Phys. Rev. E* **61**, 3712.

Brown, R. [1998] "Approximating the mapping between systems exhibiting generalized synchronization" *Phys. Rev. Lett.* **81**, 4835.

Chen, J., Lu, J.-A., Wu, X. & Zheng, W. X. [2009] "Generalized synchronization of complex dynamical networks via impulsive control" *Chaos* **19**, 043119.

Dmitriev, B. S., Hramov, A, E., Krasovskii, A. A., Starodubov, A. V., Trubetskov, D. I. & Zharkov, Y. D. [2009] "First experimental observation of generalized synchronization phenomena in microwave oscillators" *Phys. Rev. Lett.* **107**, 074101.

Earn, D. T. D., Rohani, P. & Grenfell, B. T. [1998] "Persistence, chaos and synchrony in ecology and epidemiology" *Proc. R. Soc. London, Ser. B* **265**, 1471.

Farmer, S. F. [1998] "Rhythmicity, synchronization and binding in human and primate motor systems" *J. Physiol.* **509**, 3.

Gakkhar, S. & Singh, A. [2010] "A delay model for viral infection in toxin producing phytoplankton and zooplankton system" *Commun. Nonlinear Sci. Numer. Simul.* **15**, 3607.

Grenfell, B. T., Bjornstad, O. N. & Kappey, J. [2001] "Travelling waves and spatial hierarchies in measles epidemics" *Nature (London)* **414**, 716.

Guan, S., Wang, X., Gong, X., Li, K. & Lai, C.-H. [2009] "The development of generalized synchronization on complex networks" *Chaos* **19**, 013130.

Guan, S., Gong, X., Li, K., Liu, Z. & Lai, C.-H. [2010] "Characterizing generalized synchronization in complex networks" *New J. Phys.* **12**, 073045.

Hopfield, J. J. [1982] "Neural networks and physical systems with emergent collective computational abilities" *Proc. Natl. Acad. Sci. U.S.A.* **79**, 2554.

Hu, A., Xu, Z. & Guo, L. [2010] "The existence of generalized synchronization of chaotic systems in complex networks" *Chaos* **20**, 013112.

Hung, Y. C., Huang, Y. T., Ho, M. C. & Hu, C. K. [2008] "Paths to globally generalized synchronization in scale-free networks" *Phys. Rev. E* **77**, 016202.

Ikeda, K., Daido, H. & Akimoto, O. [1980] "Optical turbulence: Chaotic behavior of transmitted light from a ring cavity" *Phys. Rev. Lett.* **45**, 709.

Kocarev, L. & Parlitz, U. [1996] "Generalized synchronization, predictability, and equivalence of unidirectionally coupled dynamical systems" *Phys. ReV. Lett.* **76**, 1816.

Koronvskii, A, A., Moskalenko, I, O. & Hramov, A. E. [2011] "Nearest neighbors, phase tubes, and generalized synchronization" *Phys. Rev. E* **84**, 037201.

Lakshmanan, M. & Senthilkumar, D. V. [2010] *Dynamics of Nonlinear Time-Delay Systems* (Springer, Berlin).

Mackey, M. C. & Glass, L. [1977] "Oscillation and chaos in physiological control systems" *Science* **197**, 287.

Maraun, D. & Kurths, J. [2005] "Epochs of phase coherence between El Niño/Southern oscillation and Indian monsoon" *J. Geophys. Res. Lett.* **32**, L15709.

Marwan, N., Romano, M. C., Thiel, M. & Kurths, J, [2005] "Recurrence plots for the analysis of complex systems," *Phys. Rep.* **438**, 237-329.

Meng, J. & Wang, X. [2007] "Robust anti-synchronization of a class of delayed chaotic neural networks" *Chaos* **17**, 023113.

Moskalenko, O. I., Koronovskii, A. A., Hramov, A. E. & Boccaletti, S. [2012] "Generalized synchronization in mutually coupled oscillators and complex networks" *Phys. Rev. E* **86**, 036216.

Moskalenko, O. I., Koronovskii, A. A. & Hramov, A. E. [2010] "Generalized synchronization of chaos for secure communication: Remarkable stability to noise" *Phys. Lett. A* **374**, 2925.

Murali, K. & Lakshmanan, M. [1998] "Secure communication using a compound signal from generalized synchronizable chaotic systems" *Phys. Lett. A.* **241**, 303.

Packard, N. H., Crutchfield, J. P., Farmer, J. D. & Shaw, R. S. [1980] "Geometry from a time series"

Phys. Rev. Lett. **45**, 712.

Parlitz, U., Junge, L., Lauterborn, W. & Kocarev, L. [1996] "Experimental observation of phase synchronization" *Phys. Rev. E* **54**, 2115.

Parlitz, U., Junge, L. & Kocarev, L. [1997] "Subharmonic entrainment of unstable periodic orbits and generalized synchronization" *Phys. Rev. Lett.* **79**, 3158.

Pecora, L. M., Carroll, T. L., Jhonson, G. A. & Mar, D. J. [1996] "Fundamentals of synchronization in chaotic systems, concepts, and applications." *Chaos* **7**, 520.

Pikovsky, A. S., Rosenblum, M. G. & Kurths, J. [2001] *Synchronization - A Unified Approach to Nonlinear Science* (Cambridge University Press, Cambridge, England).

Pyragas, K. [1996] "Weak and strong synchronization of chaos" *Phys. Rev. E* **54**, 4508(R).

Rogers, E. A., Kalra, R., Schroll, R. D., Uchida, A., Lathrop, D. P. & Rajarshi Roy [2004] "Generalized synchronization of spatiotemporal chaos in a liquid crystal spatial light modulator" *Phys. Rev. Lett.* **93**, 084101.

Rulkov, N. F., Sushchik, M. M., Tsimring, L. S. & Abarbanel, H. D. I. [1995] "Generalized synchronization of chaos in directionally coupled chaotic systems" *Phys. Rev. E* **51**, 980.

Schäfer, C., Rosenblum, M. G., Kurths, J. & Abel, H. H. [1998] "Heartbeat synchronized with ventilation" *Nature (London)* **392**, 239.

Schumacher, J., Haslinger, R. & Pipa, G. [2012] "Statistical modeling approach for detecting generalized synchronization" *Phys. Rev. E* **85**, 056215.

Sebe, J. Y., van Berderode, J. F., Berger, A. J. & Abel, H. H. [2006] "Inhibitory Synaptic Transmission Governs Inspiratory Motoneuron Synchronization" *J. Neurophysiol* **96**, 391.

Senthilkumar, D. V., Lakshmanan, M. & Kurths, J. [2006] "Phase synchronization in time-delay systems" *Phys. Rev. E* **74**, 035205(R).

Senthilkumar, D. V., Lakshmanan, M. & Kurths, J. [2007] "Transition from phase to generalized synchronization in time-delay systems" *Chaos* **18**, 023118.

Senthilkumar, D. V., Suresh, R., Lakshmanan, M. & Kurths, J. [2013] "Global generalized synchronization in networks of different time-delay systems" *Europhys. Lett.* **103**, 50010.

Shahverdiev, E. M. & Shore, K. A. [2009] "Generalized synchronization in laser devices with electro-optical feedback" *IET Optoelectron.* **3**, 274.

Shang, Y., Chen, M. & Kurths, J. [2009] "Generalized synchronization of complex networks" *Phys. Rev. E* **80**, 027201.

Sorino, M. C., Guy Van der Sande, Fischer, I. & Mirasso, C. R. [2012] "Synchronization in Simple Network Motifs with Negligible Correlation and Mutual Information Measures" *Phys. Rev. Lett.* **108**, 134101.

Stein, K., Timmermann, A. & Schneifer, N. [2011] "Phase synchronization of the El-Niño-Southern oscillation with the annual cycle" *Phys. Rev. Lett.* **107**, 128501.

Suresh, R., Srinivasan, K., Senthilkumar, D. V., Raja Mohamed, I., Murali, K., Lakshmanan, M. & Kurths, J. [2013] "Zero-lag synchronization in coupled time-delayed piecewise linear electronic circuits" *Eur. Phys. J. Special Topics* **222**, 729.

Uchida, A., McAllister, R., Meucci, R. & Rajarshi Roy, [2003] "Generalized synchronization of chaos in identical systems with hidden degrees of freedom" *Phys. Rev. Lett.* **91**, 174101.

Van Leeuwen, P., Geue, D., Thiel, M., Cysarz, D., Large, S., Romano, M. C., Wessel, N., Kurths, J. & Grönemeyer, D. H. [2009] "Influence of paced maternal breathing on fetalmaternal heart rate coordination" *Porc. Natl. Acad. Sci. USA* **106**, 13661.

Zheng, Z., Wang, X. & Cross, M. C. [2002] "Transitions from partial to complete generalized synchronizations in bidirectionally coupled chaotic oscillators" *Phys. Rev. E* **65**, 056211.

Zheng, Z. & Hu, G. [2000] "Generalized synchronization versus phase synchronization" *Phys. Rev. E* **62**, 7882.

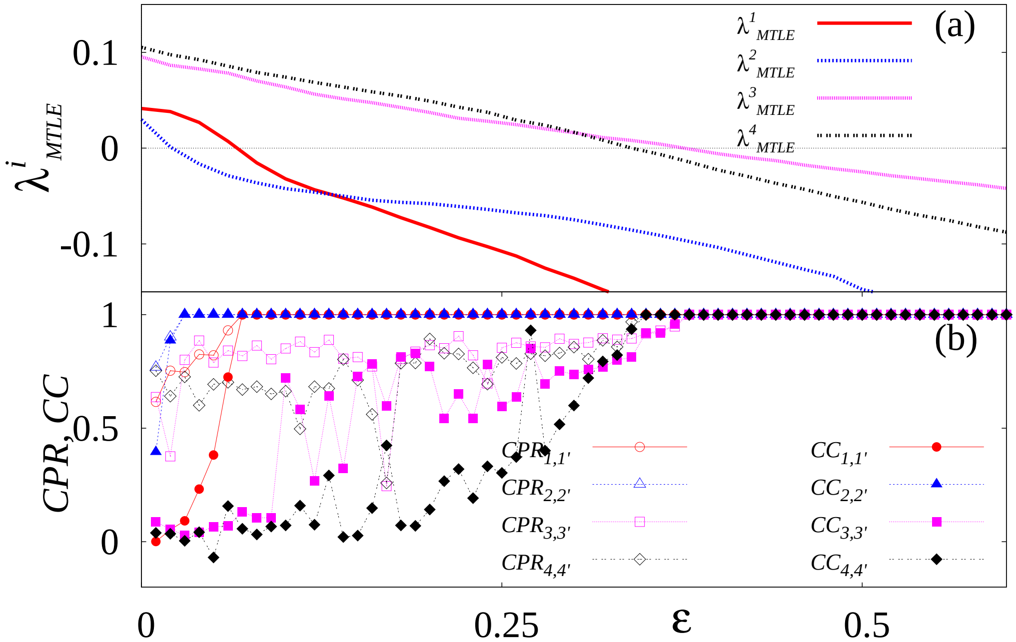

(a)
λ^i_{MTLE}
λ^1_{MTLE}
λ^2_{MTLE}
λ^3_{MTLE}
λ^4_{MTLE}
0.1
0
-0.1
(b)
CPR,CC
$CPR_{1,1'}$
$CPR_{2,2'}$
$CPR_{3,3'}$
$CPR_{4,4'}$
$CC_{1,1'}$
$CC_{2,2'}$
$CC_{3,3'}$
$CC_{4,4'}$
1
0.5
0
0.25
0.5
ε

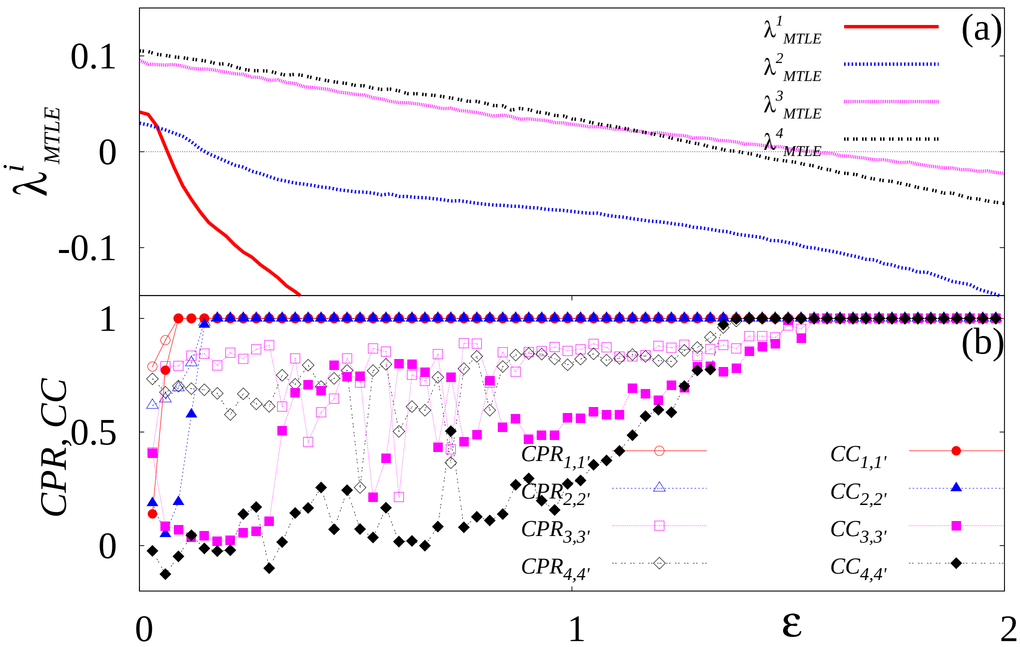

(a)
(b)
λ^i_{MTLE}
λ^1_{MTLE}
λ^2_{MTLE}
λ^3_{MTLE}
λ^4_{MTLE}
CPR, CC
$CPR_{1,1'}$
$CPR_{2,2'}$
$CPR_{3,3'}$
$CPR_{4,4'}$
$CC_{1,1'}$
$CC_{2,2'}$
$CC_{3,3'}$
$CC_{4,4'}$
ε
0.1
0
-0.1
1
0.5
0
0
1
2